Nano Today 13 (2017) 77–96

Contents lists available at ScienceDirect

Nano Today

journal homepage: www.elsevier.com/locate/nanotoday

Review

Frontiers of on-surface synthesis: From principles to applications

Qian Shen[a,b,c], Hong-Ying Gao[a,b], Harald Fuchs[a,b,c,*]

[a] Physikalisches Institut, Westfälische Wilhelms-Universität, Wilhelm-Klemm-Straße 10, 48149 Münster, Germany
[b] Center for Nanotechnology, Heisenbergstraße 11, 48149 Münster, Germany
[c] Key Laboratory of Flexible Electronics (KLOFE) & Institute of Advanced Materials (IAM), Jiangsu National Synergetic Innovation Center for Advanced Materials (SICAM), Nanjing Tech University (NanjingTech), 30 South Puzhu Road, Nanjing 211816, China

ARTICLE INFO

Article history:
Received 23 December 2016
Received in revised form 3 February 2017
Accepted 20 February 2017
Available online 18 March 2017

Keywords:
On-surface synthesis
Nanoarchitectures
Scanning tunneling microscopy
Atomic force microscopy

ABSTRACT

On-surface synthesis is the bottom-up construction of covalent bonds between molecular building blocks, which has been greatly developed during the past decade. Dozens of reactions have been successfully realized and scrutinized on various surfaces with the help of surface science techniques combined with theoretical calculations. Functional nanoarchitectures such as one-dimensional nanowires, nanoribbons and two-dimensional nanonetworks have been constructed on surfaces and explored in several potential applications. In fact, the generation of multilevel nanostructures will play a key role in future soft nanoscience and technologies due to their emergent properties ranging far beyond those of the individual molecules building them up. In this review, we discuss selected examples of important processes in on-surface synthesis developed in recent years and summarize them under the following aspects: (1) on-surface reactions in a category of different carbon types; (2) techniques applied in on-surface synthesis; (3) on-surface synthesized functional nanostructures; and (4) potential applications of on-surface synthesized nano-materials. The review concludes with a perspective of the future development of on-surface synthesis.

Contents

* Corresponding author at: Physikalisches Institut, Westfälische Wilhelms-Universität, Wilhelm-Klemm-Straße 10, 48149 Münster, Germany.
E-mail address: fuchsh@uni-muenster.de (H. Fuchs).

http://dx.doi.org/10.1016/j.nantod.2017.02.007

Introduction

A controllable construction of nanoarchitectures with atomic resolution is a fascinating concept of modern nanotechnology. Thus, novel materials with fancy properties and functions can be designed and synthesized with atomic precision. Zero-dimensional (0D) quantum dots, one-dimensional (1D) polymers or nanoribbons and two-dimensional (2D) nanosheets have been synthesized in solution or in top-down methods and applied for various applications. However, the construction of molecular electronic and spintronic devices requires the controllable arrangement and connections between the molecular counterparts in a clean environment, which is a great challenge for the materials synthesized in solution. In addition, for the top down methods such as photolithography or plasma treatment, the structural latitudes and the quality of edge structures which play vital roles in the properties of the synthesized materials are difficult to control at the atomic scale. Self-assembly of functional organic molecules on surfaces in ultra-high vacuum (UHV) stands for one of the most powerful bottom-up strategies toward the controllable construction of functional nanoarchitectures. Self-assembly structures are stabilized by weak or strong molecular interactions. The weak molecular interactions such as hydrogen bonds and van der Waals interaction have been intensively studied for several decades and a large knowledge about controlling the structure order of the molecular systems on surfaces has been accumulated. However, the lack of stability for these weakly interconnected self-assembly structures strongly limits their real applications, in particular under ambient conditions. Thus, the strong molecular interactions such as covalent or coordinated bonds in the self-assembly structures are highly important and in a strong motivation for research.

As a versatile bottom-up strategy for the construction of covalent bonds between molecular building blocks, on-surface synthesis has gained strongly increasing research attention during the past decade. Plenty of classic organic reactions have been successfully realized on single crystal surfaces in UHV, such as Ullmann coupling [1–7], Glaser coupling [8–10], Bergman reaction [11,12], aryl–aryl dehydrogenation [13–19], Diels–Alder reaction [20], Schiff-base reaction [21–24], boronic acid condensation [25–28], etc. Strong covalent bonds have been realized by homo- and hetero-coupling between alkyl, alkenyl, alkynyl, aryl and other functional groups at mild conditions. Naturally, 1D covalent or organometallic polymers, 2D molecular networks and novel materials with special configurations such as nanoribbons have been synthesized directly on surfaces with atomic precision and fine-tuned structures. Their reaction mechanisms have also been revealed by the capture of the intermediate states, which are stabilized by the metal surfaces and controlled sample temperatures. The structures of the final products are dominated by the design of the molecular precursors and influenced by other conditions such as the chemical nature and lattice structures of the underlying substrates. These new materials have shown great potentials in various applications. For example, electronic [1] and spintronic devices [29] were constructed by a controllable coupling of molecular counterparts. Highly efficient catalysts were synthesized by isolating active metal centers in designed 2D coordinated metal–organic frameworks [30].

In this review, we will summarize and classify the on-surface reactions by a category of reactions between different SP-orbitals of carbon: SP^0-C (carbene), SP^1-C (alkynyl), SP^2-C (aryl and alkenyl), SP^3-C (alkyl halide and linear alkane), and other bond formations based on chemical groups containing C—O or C═O (carboxylic acid/acetyl/ether), etc. Techniques involved in these studies such as scanning tunneling microscopy (STM) and atomic force microscopy (AFM) will be introduced. The architectures built by on-surface synthesis and their further applications will be discussed. Finally, a perspective of the differing development directions of on-surface synthesis will be given.

Summary of various on-surface reactions

In the past decade, traditional in-solution and gas-phase organic synthesis has been extended to single crystal surfaces in UHV environment. With the help of STM and AFM, the molecular structures and properties of the reactants and the final products can be characterized with atomic resolution. More importantly, high reactivity intermediate states with short lifetimes can be stabilized by surfaces at cryostat temperatures and captured by STM and AFM, providing a deeper insight on the reaction mechanisms. Tireless efforts have been made to control the on-surface reaction pathways as well as their outcomes. The influences of the chemical structures of the precursors and the underlying surfaces to the on-surface reactions have also been scrutinized. It has been proved that in most cases the surfaces are not only used to support the reactions, but also can serve as reaction catalysts or directly participate reactions via organometallic states. Up to now, the on-surface reactions based on carbene [31–33] (SP^0-C), alkynyl [8,9,12,35,36,38] (SP^1-C), aryl [1–3,16,18,19] and alkenyl [20,44] (SP^2-C) groups, the activation of alkyl halide [46] and linear alkane [47] (SP^3-C), the homocoupling between carboxylic acid groups (C═O) [48,49], the reactions containing acetyl [50] and other [51] groups (C—O) have all been reported. Schiff-base reactions [21–23] and condensation of boronic acids [25,26,56] which introduce dopants such as nitrogen and boron atoms to the synthesized nanostructures, have also been used to build up covalently linked architectures on surfaces. Here, based on the electronic orbital classification of carbon, the carbon–oxygen and other bonding cases toward covalent connection, we will classify the reported works (Table 1). Within this framework, some representative results are presented in details below.

On-surface reactions based on SP^0-C

As an alternative to thiol-based ligands, N-heterocyclic carbenes (NHCs) have been used to form high quality self-assembly monolayers (SAMs) on gold surfaces, which have significant applications in sensing, surface protection, electrochemistry, nanoelectronics and drug delivery [57,58]. Compared with the thermal and oxidative instability of thiol-based SAMs, the bonds between NHCs and gold atoms are strong enough to endure high temperatures, organic solvents, pH extremes, electrochemical cycling above 0 V and 1% hydrogen peroxide [33]. To improve the ordering of the SAMs based on carbenes, Wang et al. [32] studied the microscopic mechanism

Table 1
Summarize and classify on-surface reaction types.

Category	Reaction name	Chemical equation	Ref.
SP^0-C	N-heterocyclic carbenes formation and dimerization	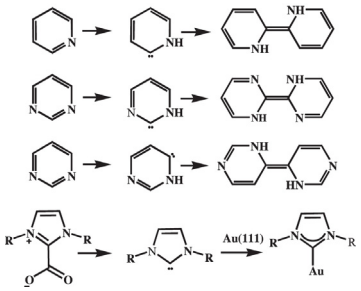	[31–33]
SP^1-C	Glaser coupling		[8–10]
	Alkyne cyclotrimerization	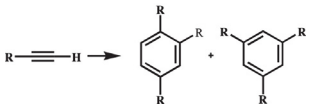	[34,35]
	Metalated carbyne	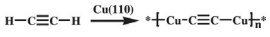	[36]
	Bergman reaction	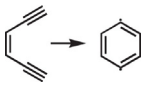	[11,12]
	Azide–alkyne cycloaddition	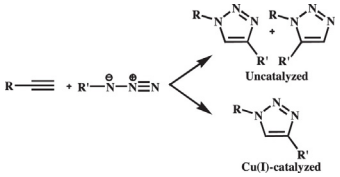	[37,38]
	Sonogashira coupling	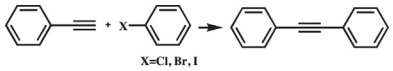	[39,40]
	Dehalogenative homocoupling of terminal alkynyl bromides	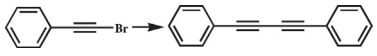	[41]
SP^2-C	Ullmann coupling	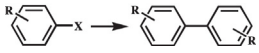	[1–3,42]
	Aryl–aryl dehydrogenation coupling	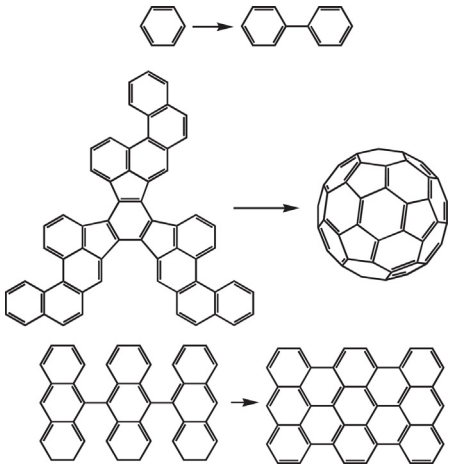	[16,18,19,42,43]
	Dehydrogenative homocoupling of terminal alkene	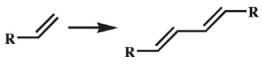	[44]

Table 1 (*Continued*)

Category	Reaction name	Chemical equation	Ref.
	Dehalogenative homocoupling of terminal alkenyl bromides	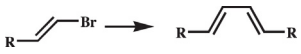	[45]
	Diels–Alder reaction	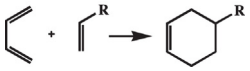	[20]
SP^3-C	Wurtz coupling		[46]
	Linear alkane polymerization	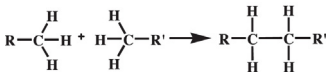	[47]
Carboxylic acid/ester/ether/acetyls (C—O, C=O)	Decarboxylative polymerization	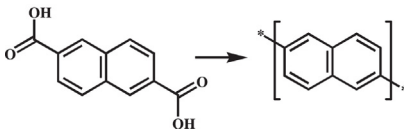	[48]
	Dehydrogenative coupling	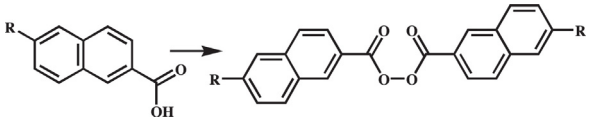	[49]
	Dimerization and cyclotrimerization of acetyls	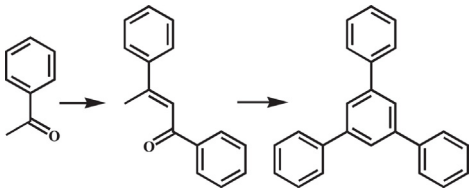	[50]
	Dealkylation of ethers to alcohols		[51]
	Reduction	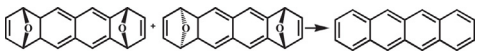	[52]
	Schiff-base reaction (imine formation)	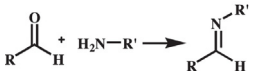	[21–24]
Others	Boronic acid condensation	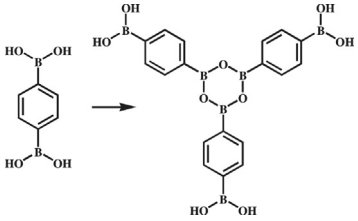	[25,27,53]
	Surface confined Metal–organic coordination	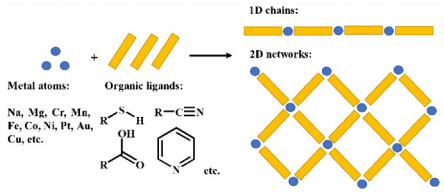	[54,55]

of the self-assembly process of carbenes and demonstrated the ballbot-type motion of NHCs on Au(111). The reaction process was illustrated in Fig. 1a. Gold atoms could be extracted from the surface by NHCs and the complex had a high desorption barrier and surface mobility, which enabled the formation of highly ordered and stable SAMs. Fig. 1b showed the successive STM images taken in the same area of low-coverage IPr molecules on Au(111), clearly demonstrated the high on-surface mobility. Theoretical simulation confirmed the IMe–Au complex formation and migration on Au(111), as shown in Fig. 1c.

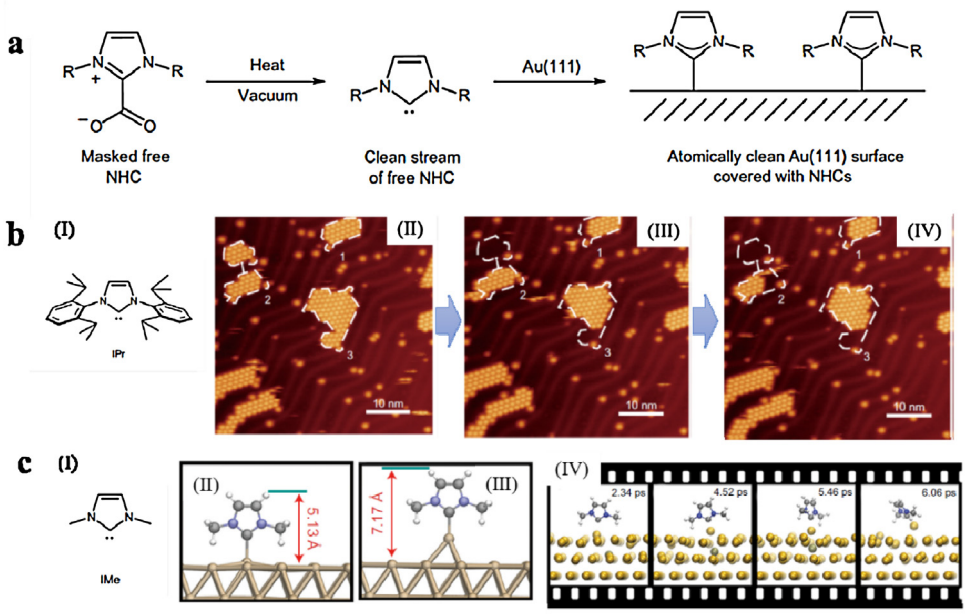

Fig. 1. On-surface synthesized NHCs (SP^0-C). (a) Schematic illustration of the formation of NHCs on gold. (b) The chemical formula of IPr NHC (I) and the successive STM images of IPr–Au islands on Au(111) (II–IV). (c) The chemical formula of IMe NHC (I) and the simulated structures of IMe NHC without (II) and with (III) an Au adatom. (IV) CP–MD simulated procedure of the formation and migration of IMe–Au complex on Au(111). Copyright© 2016 Nature Publishing Group, reprinted with permission from Ref. [32].

On-surface reactions based on SP^1-C

Homocoupling of terminal alkynes (Glaser coupling), which offers π-conjugated structures and has volatile H_2 as the only by-product, have been widely studied to build 1D and 2D nanostructures on surfaces. In 2012, Zhang et al. [8] reported the first attempt of Ag surface-mediated terminal alkyne C—H activation and realized the homocoupling of alkynes. Small covalently linked 2D structures up to 10 nanometers were synthesized on surfaces in UHV under mild conditions. The reaction pathway was studied by STM and DFT calculations. In 2013, Gao et al. [9,59] showed the synthesis of 1D graphdiyne wires by on-surface Glaser coupling (Fig. 2a). Side reactions occurred simultaneously with Glaser coupling and significantly lowered the structure regularity. By introducing long side groups to the backbones of the precursors, the effect of steric hindrance successfully restrained the unwanted reactions and urged the formation of long π-conjugated linear polymers on surfaces. Another efficient way to increase the reaction selectivity is using surface structures, for example the step edges, as templates. Upon alignment at the step edges of the Ag(877) vicinal surfaces, the chemoselectivity of Glaser coupling is dramatically increased and 1D polymers over 30 nm long were synthesized [10]. Sun et al. [41] delicately designed and synthesized molecular precursors with one, two, and three alkynyl groups to build up dimers, 1D and 2D nanostructures on Au(111) respectively, with corresponding organometallic stages observed, offering an alternative and efficient way to synthesize nanoarchitectures with acetylenic scaffolds. The chemical nature and the lattices of the underlying surfaces can also influence the reaction pathways. Gao et al. [9] proved that Glaser coupling is most efficient on Ag(111) surface, compared with Au(111) and Cu(111) surfaces. Liu et al. [60] reported that on Ag(111) the dominant reaction of 2,5-diethynyl-1,4-bis(phenylethynyl)-benzene was Glaser coupling, while on Ag(110) and Ag(100), organometallic nanostructures were the main products. Apart from thermal activation, Gao et al. [61] showed that Glaser coupling could also be triggered by light, thus opening new opportunities for on-surface synthesis of conjugated nanostructures at mild conditions.

Surprisingly, the same precursors reported by Zhang et al. [8] went through cyclotrimerization on Au(111), which is a two-step [2+2+2] cyclization reaction. Upon annealing, regular 2D covalently bonded polyphenylene nanostructures were synthesized with high selectivity [34]. Linear precursor diyne was also reported to go through cyclotrimerization process on Au(111) [35], implying that the chemical nature of the surfaces may alter the preferred reaction pathways.

Carbyne, a 1D chain of carbon atoms, is one of the carbon allotropes which is as important as fullerene, graphene and carbon nanotube. Although extraordinary physicochemical properties have been predicted about carbyne and its metalated counterpart, their stability issue and challenging synthesis with well-defined structures hampered their further applications. Sun et al. [36] reported the successful synthesis of 1D metalated carbyne chains with submicron scale length (up to ~120 nm) on Cu(110) at ~450 K through the dehydrogenative coupling of ethyne molecules (Fig. 2b). The Cu(110) surface acted as the reaction catalysis and the 1D template.

Bergman cyclization is the rearrangement reaction of enediyne. On-surface Bergman cyclization was first reported by Sun and co-workers [12]. Followed by radical polymerization. 1D conjugated nanostructures were synthesized by Bergman cyclization on Cu(110) surfaces (Fig. 2c).

Azide–alkyne 1,3-dipolar cycloaddition is a classical "click reaction". When this reaction is performed at high temperatures without catalysts, it produces a mixture of 1,5- and 1,4-triazole regioisomers. When solvated Cu(I) ions are used as catalysts, it will provide 1,4-triazoles with high yield and regioselectivity under ambient conditions (CuAAC reaction). This reaction which is byproduct free and triggered with little thermal activation, has great potential to be realized on surface. Since copper is a good catalyst for this reaction, Bebensee and co-workers [37] first tested the coupling reactions between 9-ethynylphenanthrene (alkyne) and 4-azidobiphenyl (azide) on Cu(111). The two precursors were designed to be able to endure thermal sublimation and can be distinguished by STM. The reaction did happen on surfaces with the 1,4-regiosiomer as the only product, but the yield was quite

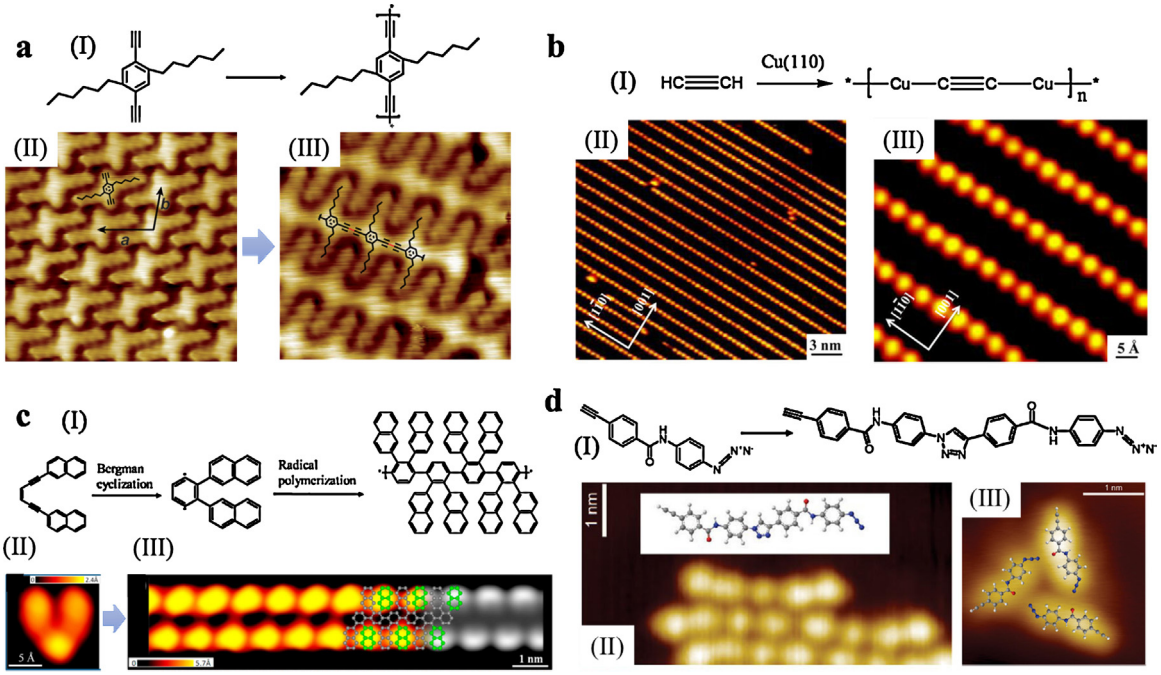

Fig. 2. Examples of on-surface reactions based on SP^1-C. (a) An example of Glaser coupling. (I) Chemical equation of on-surface Glaser coupling. (II) High-resolution STM image of alkyne precursors on Au(111) (6 nm × 6 nm). (III) High-resolution STM image of the 1D arylalkyne polymers on Au(111) after thermal treatment (5 nm × 5 nm). Copyright© 2013 WILEY-VCH Verlag GmbH & Co. KGaA, Weinheim, reprinted with permission from Ref. [9]. (b) On-surface synthesis of metalated carbyne. (I) Schematic illustration of the reaction procedure. Large scale (II) and high-resolution (III) STM images of the metalated carbyne chains. Copyright© 2016, American Chemical Society, reprinted with permission from Ref. [36]. (c) 1D polyphenylene chains synthesized by on-surface Bergman reaction. (I) Schematic illustration of Bergman cyclization and the following radical polymerization. (II) High-resolution STM image of a single precursor molecule. (III) High-resolution STM image of the synthesized polyphenylene chain and a DFT-based STM simulation (greyscale part), superimposed with an equivalently scaled structure model. Copyright© 2013, American Chemical Society, reprinted with permission from Ref. [12]. (d) On-surface azide–alkyne cycloaddition on Au(111). (I) Schematic illustration of the reaction process. (II) STM images of dimers and trimers formed by azide–alkyne cycloaddition (3.5 nm × 7 nm). The inset is the molecular structure model of a dimer. (III) High-resolution STM image of the triangular self-assembly structure of monomers, with an equivalently scaled model superimposed (3 nm × 3 nm). End groups facing each other would prevent the reaction. Copyright© 2013, American Chemical Society, reprinted with permission from Ref. [38].

low, which was explained by the decomposition of the azide reactants. A direct surface-catalyzed reaction pathway without Cu was investigated by Díaz Arado et al. [38] (Fig. 2d). They performed an azide–alkyne 1,3-dipolar cycloaddition on Au(111) by choosing N-(4-azidophenyl)-4-ethynylbenzamide molecules as precursors, which can be thermally deposited and diffuse on surface to react with each other. The reaction happened at room temperature and provided only 1,4-regioisomers. DFT calculations proved that the Au(111) surface did not serve as a catalyst for the reaction, but rather as a 2D-restraint to the reactants. The regioselectivity of the azide–alkyne cycloaddition came from the surface constraint effect based on the chemical design of the reactants, which introduced a steric hindrance for the 1,5-regioisomer.

On-surface reaction based on SP^2-C

The Ullmann reaction, the homo-coupling reaction between aryl halides, is the most popular reaction in on-surface synthesis. As an important way to link aromatic units through C—C bonds, it has been widely employed to build up all sorts of carbon-based scaffolds on coinage surfaces, from dimers, 1D polymer chains to 2D covalently linked organic networks. Organometallic nanostructures, as intermediate states of the Ullmann coupling, have also been achieved on surfaces.

In 2000, Hla et al. [62] reported the on-surface Ullmann coupling reaction between individual iodobenzene molecules induced by multistep STM manipulations in a controlled manner: the iodine atoms were firstly separated from the reactants by tunneling electrons, then the remaining phenyls were brought together by lateral manipulation, and the final chemical welding was mediated by tunneling electrons to form biphenyl molecules on Cu(111). This work not only demonstrated the feasibility of on-surface Ullmann reaction, but also demonstrated the feasibility for the controlled construction of individual molecules on predefined surface locations.

The pioneering work done by Grill and co-workers [2] in 2007 demonstrated for the first time that the porphyrin molecules with bromine substitutions can be connected by Ullmann reaction under thermal treatment. By tailoring the chemical structure of the building blocks, the numbers and positions of the connection points could be controlled, and various artificial structures such as dimers, linear chains and 2D networks were achieved on gold surfaces. By annealing NiTBrPP molecules on Au(111) at 525 K, a robust, extended 2D porphyrin network was achieved. Various characterization techniques, such as STM, X-ray absorption, core-level photoemission, and microbeam low-energy electron diffraction, were combined to reveal the reaction mechanism [63]. However, the lack of long-range order haunts the on-surface synthesized 2D structures, hampering their further application. By taking advantages of the bond energy differences between C—Br and C—I bonds, Lafferentz et al. [3] succeeded in connecting porphyrin building blocks in a hierarchical manner by sequential activation (Fig. 3a). The dissociation of C—I bonds happened at lower temperatures, forming 1D polymer chains which preserved flexibility at the surfaces during the subsequent thermal activation at higher temperatures, thus increasing the regularity of hierarchical synthesized 2D networks. Substrate directed growth was also discussed by comparing the results on Au(111) with the anisotropic Au(100) surfaces. This “molecular zipper” method for the on-surface construction of covalently linked networks with high regularities was

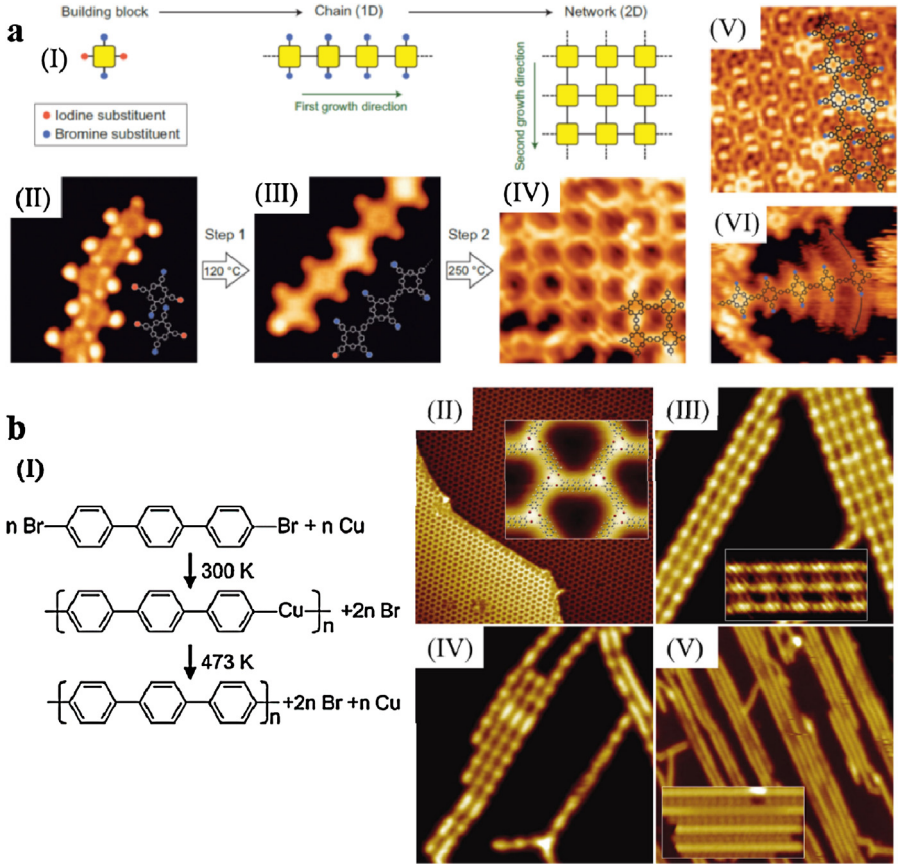

Fig. 3. Examples of on-surface Ullmann reaction. (a) Hierarchical growth of 2D nanostructures with high regularity. (I) Schematic illustration of the sequential activation procedure. (II) STM images (8 nm × 8 nm) of the self-assembly structure of *trans*-Br_2I_2TPP molecules on Au(111). (III) STM images (8 nm × 8 nm) of a polymer chain after the first-step reaction. A close-packed polymer island shown in (V) (10 nm × 10 nm). (IV) STM images (10 nm × 10 nm) of a covalently linked 2D network after two steps reaction. (VI) STM image (12 nm × 10 nm) of a polymer chain fixed at the one end and moving on the other. Copyright© 2012, Nature Publishing Group, reprinted with permission from Ref. [3]. (b) Organometallic intermediate states of on-surface Ullmann coupling. (I) Schematic illustration of Ullmann coupling reaction via the organometallic intermediate. (II) STM image of the self-assembly structure of precursors at 77 K. (III) STM image of the organometallic intermediate stages after annealing the sample to 300 K. (IV) STM image of the sample annealed to 393 K. (V) STM image of the poly(para-phenylene) oligomers after annealing the sample to 473 K. Copyright© 2011, American Chemical Society, reprinted with permission from Ref. [4].

also utilized by Lin et al. [64]. By choosing bifunctional precursors which contained both pyridyl and C—Br groups, they got linear structures through pyridyl–Cu–pyridyl coordination at room temperature prior to activating the C—Br bonds at 180 °C. The linear chains were connected laterally through Ullmann reaction, forming 2D structures with high regularity on Au(111). The influences of the underlying surfaces to the regularities of the 2D structures were studied by comparing the homocoupling results between the hexaiodo-substituted macrocycle cyclohexa-m-phenylene molecules on Au(111), Ag(111) and Cu(111) [5]. By varying the diffusion mobility and the reactivity, the chemical nature of the substrates could impose significant impact to the reaction outcomes. On Cu(111), the energy barrier for diffusion was much higher than that for covalent bond formation, resulting in open branched networks. While on Ag(111), the reverse relation between diffusion and reaction holds, highly ordered structures were synthesized. Therefore, by deliberately designing the molecular precursors, properly selecting the substrates and carefully controlling the kinetics of the reactions, it is highly likely to get large scale well-defined covalently linked 2D structures on surfaces.

Numerous efforts have also been devoted to the construction and physical property characterization of 1D structures synthesized by Ullmann coupling. One famous example was displayed by Lafferentz and co-workers [1] in 2009, who synthesized polyfluorene wires by on-surface Ullmann coupling and measured their length dependent conductance by pulling a single wire up from the Au(111) surface with an STM tip. By introducing a stepped surface Au(10, 7, 7) as the substrate, the thermal induced Ullmann reaction of α,ω-dibromoterfluorene molecules was explored by Sywell et al. [65]. STM results demonstrated that the kinks were the active sites in the catalytic process and the synthesized polymers aligned along the step edges. Besides the surface structures, Koch et al. [66] demonstrated that the chemical nature of the substrates influenced the Ullmann reaction results dramatically. It could not only alter the activation energy of Ullmann coupling but also differ the reaction pathways. By exploring the thermal induced reactions of dibromohexabenzocoronene (Br_2-HBC) on Au(111) and Cu(111), they proved that Ullmann coupling was induced at 520 K on Au(111) between Br_2-HBC molecules through a radical process; while on Cu(111), organometallic chains were formed at room temperature.

Meanwhile, the organometallic intermediate states of Ullmann coupling reactions induced numerous additional investigations. Unambiguous STM images of organometallic intermediate states of Ullmann coupling were captured by Wang et al. [4] (Fig. 3b). By varying the backbones of the precursors from linear to V-shaped structures, zigzag polymer chains with C—Cu—C bonds and organometallic macrocycles were synthesized on Cu(111) [7,67]. The structural sizes could be regulated by surface templates such as Cu(110)-(2 × 1)O nano-channels [68].

Oligophenylene macrocycles were synthesized by on-surface Ullmann coupling between V-shaped precursors. By

depositing 4,4″-dibromo-m-terphenyl molecules on Cu(111) held at 550 K, ordered arrays of hyperbenzene rings with a diameter of 2.13 nm were observed. One hyperbenzene was composed of six m-terphenylene fragments, containing 18 phenylene groups [7]. Recently, a cyclotriacontaphenylene containing 30 phenylene groups was synthesized by Chen et al. [69] on Ag(111). The diameter of a macrocycle was 4.0 nm and it acted as a molecular quantum corral, confining the surface state inside, which was demonstrated by combined STS and DFT results.

Molecular nodes which are junctions where several molecular chains connected, are important components in molecular electronics. Nacci et al. [6] reported the synthesis of an non-symmetrical molecular node with three Br substitutions. Ullmann reaction was introduced to link three molecular wires to the node. Electronic characterization showed that different conjugation pathways between them offered different electronic properties. Recently the Ullmann reaction was used for 2D chirality transfer. The chirality can be preserved from the self-assembled lamellar structures of 1,4-dibromo-2,5-didodecylbenzene and 1,4-dibromo-2,5-ditridecylbenzene to oligo-p-phenylenes, offering a new way for the construction of stable chiral structures [70].

Apart from metal surfaces, Ullmann reactions can also be performed on insulating and semiconducting surfaces, such as NaCl [71], titanium dioxide [72] and molybdenum sulfide surfaces [73]. The electronic properties of molecular wires on insulating and semiconducting surfaces are of vital importance to the development of nanoelectronics, because the molecular devices will be constructed on nonconductive surfaces for applications. In 2009, Bombis and co-workers [71] synthesized long polyfluorene chains by Ullmann coupling on Au(111), then carefully deposited NaCl on the same surface at 270 K. As the area of NaCl islands increased, the polyfluorene wires would be forced to absorbed partially on the insulating surface. STS demonstrated the electronic structures of a polyfluorene wire was dependent to the local environment. In 2013, Kolmer et al. [72] demonstrated the feasibility of on-surface Ullmann polymerization on the TiO_2-(011)-(2 × 1) surface, opening new possibilities of constructing molecular devices directly on substrates with suitable bandgaps. Linear oligomers were synthesized on TiO_2 simply by thermal treatment of the molecular precursor 10,10′-dibromo-9,9′-bianthryl (DBBA). It was speculated that the reaction mechanism was a radical process, different from that on metal surfaces. More recently, the Loh Kian Ping group [73] (Singapore) succeeded in the synthesis of a new phase of substoichiometric molybdenum sulfide (s-MoS_x) on a sulfur-enriched copper substrate and tested its catalytic ability for the Ullmann coupling. 2,8-Dibromodibenzothiophene molecules were chosen as precursors and their cyclic tetramers were synthesized with high selectivity, originating from the 4-fold symmetric active sites on the basal planes of s-MoS_x.

Usually, it is difficult to connect aromatic compounds directly through aryl–aryl dehydrogenation coupling in traditional organic synthesis due to a large bond dissociation enthalpy. It usually requires transition metal catalysis and harsh conditions such as high temperatures or super acid environment and yet shows a poor reaction selectivity. When the precursors were constrained to the surfaces, the catalytic and confined effect of the underlying substrates can make the reaction happen at mild conditions. The reaction selectivity can be controlled by the precursor structure design or different reaction conditions. For example, the process of synthesizing C_{60} from commercially available starting materials requires a dozen steps. Graphite vaporization in an inert atmosphere provided an efficient but uncontrollable way of producing C_{60} and C_{70}. For higher fullerenes, such as C_{84}, the yield of the evaporation technique was very low and the following purification processes could be very difficult. In 2008, Otero et al. [19] demonstrated the efficiency of the surface-catalyzed cyclodehydrogenation method for transferring $C_{60}H_{30}$ and $C_{57}N_3H_{30}$ to the corresponding C_{60} and $C_{57}N_3$ cages on Pt(111). The reaction happened at 750 K, and the yield reached 100% (Fig. 4a). In 2010, Amsharov et al. [13] demonstrated that the surface-catalyzed cyclodehydrogenation processes did not include the C—C bond rearrangement, so the isomeric identity of fullerenes could be controlled by the precursor design. They succeeded in the on-surface synthesis of C_{84} on Pt(111) by simply annealing at 550 °C. This method was also used to produce chemically tailored nanographenes from polyphenylenes on Cu(111). Two intermediate states were stabilized on surfaces, giving unprecedented insights of the aryl–aryl dehydrogenation reaction mechanism [18].

Except for the intramolecular aryl–aryl dehydrogenation for 0D quantum dot synthesis, this reaction can also be induced between different molecules, offering an effective way to connect different organic building blocks to complex multicomponent nanostructures. Haq and co-workers [74] demonstrated that this reaction could be used as an universal strategy to connect a wide range of π-functional molecules, such as porphyrin, pentacene and perylene, to build multicomponent molecular devices directly on surfaces. STM results showed that heterostructures with diverse compositions, structures and topologies were synthesized on Cu(110). Specific products, such as block copolymers, could be controllably generated at different reaction parameters by utilizing the C—H bond energy differences. The influences of the molecular precursor structures and the surface geometries to the reaction outcomes were also discussed. Other examples of the surface-catalyzed aryl–aryl dehydrogenation processes used unsubstituted porphine [17] or tetra(mesityl)porphyrin [15] molecules on metal surfaces. Dimers, trimers, and larger oligomers were on-surface synthesized. For the tetra(mesityl)porphyrin molecules, the 4-methyl groups were demonstrated as the unique connection points. Sun et al. [43] reported the selective C—H activation and connection between quaterphenyl molecules, offering another example of on-surface aryl–aryl dehydrogenation coupling reaction. Recently Li et al. [16] reported the regioselective aromatic C—H activations on both Au(111) and Ag(111) by using hydroxyl as a directing group. The different binding strength between the phenol oxygen atoms and the surfaces resulted in the surface controlled monoselective *ortho* C—H activation on Ag(111) and diselective *ortho* C—H bond activation on Au(111) (Fig. 4b).

Alkene represents another important formation of SP^2-C. On-surface homocoupling between two terminal alkenyl groups were reported to give a *trans*-diene moiety on Cu(110), different from the dimerization products of alkenes which are usually obtained in solution [44]. *Cis*-diene was synthesized with high selectivity on Cu(110) through dehalogenative homocoupling of alkenyl bromides by Sun et al. [45]. DFT calculations demonstrated that the organometallic intermediate with *cis*-form was the most stable configuration, which was responsible for the high stereoselectivity. The Diels–Alder reaction, a cycloaddition reaction which combines a conjugated diene and a dienophile (an alkene), is an electrocyclic reaction that involves the 4 π-electrons of the diene and 2 π-electrons of the dienophile. Aragonès et al. [20] reported the tip-induced electrostatic catalysis of an on-surface Diels–Alder reaction, showing that the reaction kinetics and thermodynamics can be controlled by an external electric field. They observed a fivefold increase in the Diels–Alder reaction rate and proved that electric fields can be used as a new approach to catalyze even a non-redox chemical reaction.

On-surface reactions based on SP^3-C

The selective activation of C—H bonds of alkanes under mild conditions is very important for chemical industry. Its realization

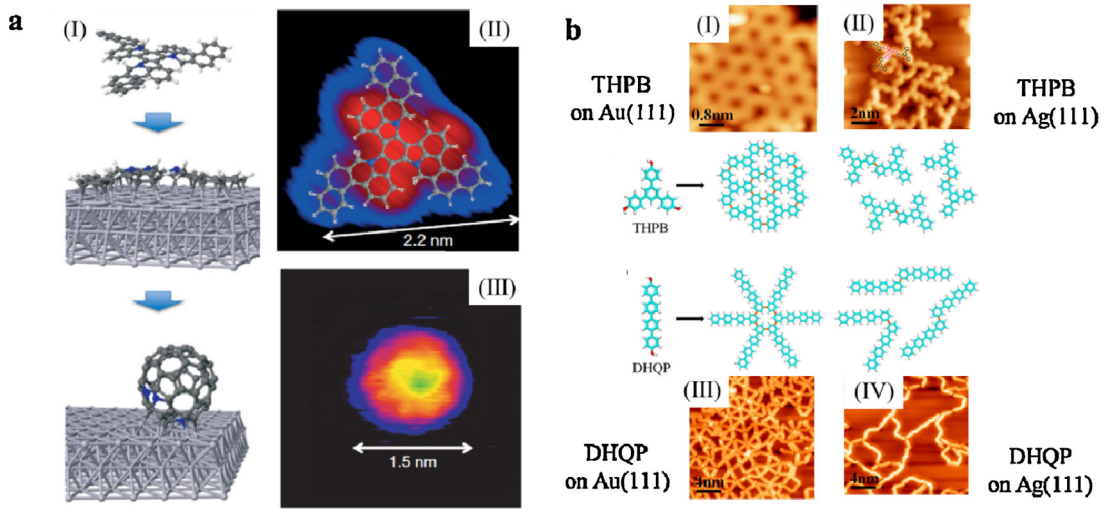

Fig. 4. On-surface aryl-aryl dehydrogenation coupling. (a) High yield C_{60} synthesis on Pt(111). (I) Geometrical structures of $C_{57}H_{33}N_3$ molecules at different stages of the reaction. (II) STM image of the $C_{57}H_{33}N_3$ molecule on Pt (111), with chemical structure superimposed. (III) STM image of an $C_{57}N_3$ molecule. Copyright© 2008, Nature Publishing Group, reprinted with permission from Ref. [19]. (b) Surface controlled regioselective aromatic C—H activation. (I) STM image of THPB on Au(111) after annealing at 340 °C. (II) STM image of THPB on Ag(111) after annealing at 300 °C. (III) STM image of DHQP on Au(111) after annealing at 320 °C. (II) STM image of DHQP on Ag(111) after annealing at 300 °C. Copyright© 2016, American Chemical Society, reprinted with permission from Ref. [16].

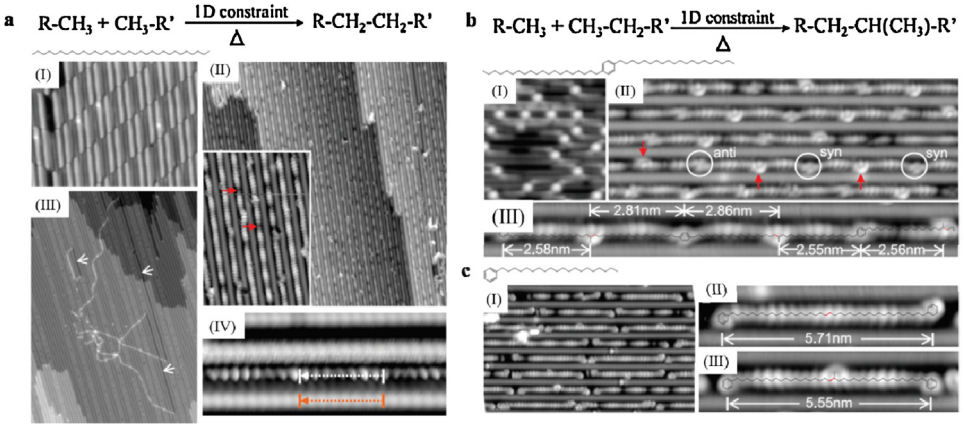

Fig. 5. Linear alkane polymerization on Au(100). (a) Dehydrogenative polymerization of n-dotriacontane ($C_{32}H_{66}$) on Au(110). (I) STM image of n-dotriacontane monomers deposited on Au(110)-(1 × 2) at 300 K. (II) Polyethylene chains formed in the Au(110)-(1 × 3) reconstruction grooves by annealing at 440 K for 30 min. (III) STM tip manipulation confirmed the covalent nature of the polymer chains. (IV) High-resolution STM image of Au atomic rows and a polyethylene chain. (b) Polymerization of 1,4-di(eicosyl)benzene (DEB) molecules. (I) DEB monomers deposited on Au(110)-(1 × 2) at 300 K. (II) Polymerized DEB chains in the Au(110)-(1 × 3) channels after annealing at 420 K for 10 h. (III) High-resolution STM image of a section of DEB polymer chain superimposed with a molecular model. (c) Dimerization of eicosylbenzene (EB) molecules. (I) Dimers of EB after annealing at 440 K for 1 h. Two types of dimers: (II) terminal C—C coupling and (III) terminal/penultimate C—C coupling with a methyl side group. Copyright© 2011, American Association for the Advancement of Science, reprint with permission from Ref. [46].

will enable to generate cheap alkanes which can be easily got from petroleum and natural gas to act as raw materials in industrial products. Unfortunately, this reaction can only be triggered at harsh conditions in solution and the molecules may undergo several competing processes, showing very poor selectivity. Zhong et al. [47] took a reconstructed anisotropic Au(110)-(1 × 2) surface as a starting template for the on-surface dehydrogenative C—C coupling of linear alkanes. The selectivity of the reactions was kinetically forced by the 1D surface reconstruction, while the Au-catalyzed dehydrogenation of the ultimate and pen-ultimate CH-groups was allowed at mild temperatures. Fig. 5a shows the self-assembly structures of *n*-dotriacontane ($C_{32}H_{66}$) on Au(110). The dehydrogenative polymerization process was triggered by annealing at 440 K and the alkane monomers were bonded end-to-end. The overall length of the polymer chains could reach 200 nm, equal to 50 monomer units. The lateral STM tip manipulations confirmed the covalent nature of the connections. The polymerization process of 1,4-di(eicosyl)benzene (DEB) molecules happened mainly between a terminal methyl group and a penultimate methylene group, and the latter case resulted in methyl branches which could be clearly distinguished in STM images (Fig. 5b). Two types of dimers were observed after thermal treatment of eicosylbenzene (EB) molecules at 440 K for 1 h, showing that the methyl C—H bonds were easier to activate than phenyl C—H bonds on surfaces, which was different from the solution cases (Fig. 5c).

Another example of SP^3-C on-surface reactions, the homocoupling of alkyl halide molecules were reported by Sun et al. [46]. This reaction could happen on Cu(110), Ag(110) and Au(111) surfaces at different temperatures, in the order of Cu(110) > Ag(110) > Au(111). DFT calculations showed three reaction steps: debromination, diffusion and coupling, among which, the rate-limiting step was the coupling process.

On-surface reactions based on carboxylic acid/ester/ether/acetyls (C—O, C=O) groups

Chemical reactions based on molecules with C—O/C=O as functional groups stand for another promising approach for

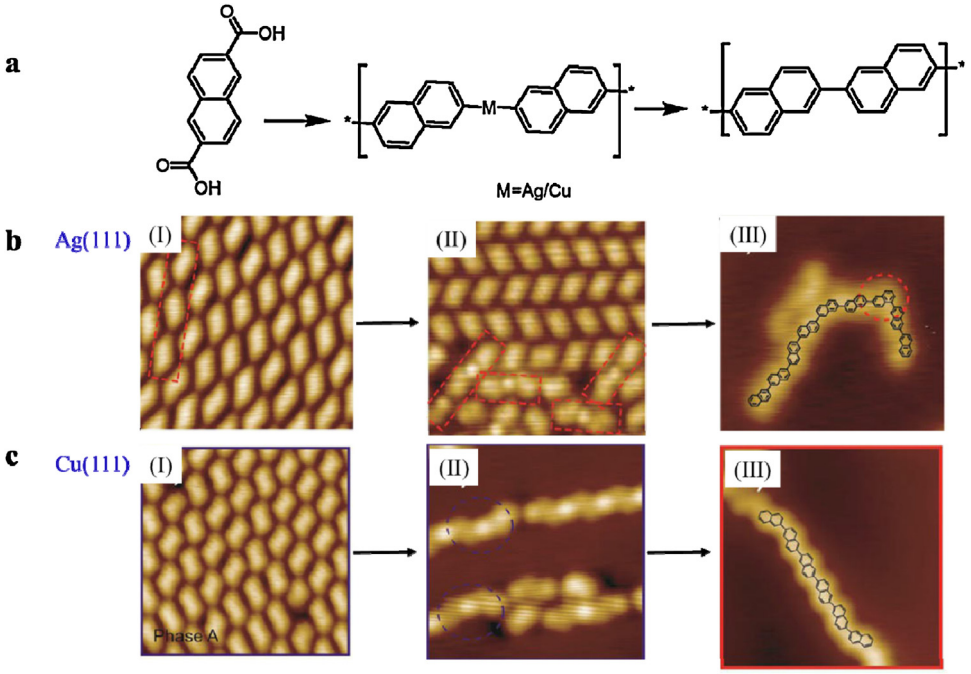

Fig. 6. On-surface decarboxylative polymerization of 2,6-naphthalenedicarboxylic acid (NDCA) on Ag(111) and Cu(111). (a) Schematic illustration of the reaction process. (b) (I) Self-assembly structure of NDCAs on Ag(111) with L-chirality (6 nm × 6 nm). (II) STM image of the reaction products of NDCAs on Ag(111) surface after annealing to 156 °C (6 nm × 6 nm). (III) STM image of C—C coupling products of NDCAs on Ag(111) after annealing to 176 °C (6 nm × 6 nm). (b) (I) One of the self-assembly phases of NDCAs on Ag(111) (6 nm × 6 nm). (II) STM image of the C—Cu—C organometallic intermediates (5 nm × 5 nm). (III) STM image of the final polymerization products of NDCAs on Cu(111) (5 nm × 5 nm). Copyright© 2014, American Chemical Society, reprint with permission from Ref. [48].

on-surface synthesis. Several reliable reactions have been applied on surfaces to build novel nanostructures: decarboxylative and dehydrogenative coupling of carboxylic acid, dimerization and cyclotrimerization of acetyls, dealkylation of ethers to alcohols, Schiff-base reaction, etc. Gao et al. [48] reported the metal-catalyzed polymerization of 2,6-naphthalenedicarboxylic acid to form poly-2,6-naphthalenes on Au(111), Ag(111), Cu(111), Cu(100) and Cu(110) surfaces (Fig. 6). Based on the intermediates observed by high resolution STM, a three-step reaction mechanism was proposed. First, metal catalyzed dehydrogenation took place at low temperature and metal–organic self-assembly structures were formed. At higher annealing temperature, polymeric bisnaphthyl-metal intermediates were observed, indicating a decarboxylation process. Upon further thermal treatment, metals were eliminated from the structures, poly-naphthalenes chains with over 50 nm length were achieved. The effects of the substrates were also discussed: Cu(111) surfaces acted as the most efficient substrate for polymerization compared with the other surfaces. The reactivity strength was laid in the following order: Cu(111) > Cu(100) > Ag(111) > Cu(110) > Au(111). Another example of on-surface reaction containing the carboxylic acid moieties was reported by the same group [49]: the aromatic acid (6-ethynyl-2-naphthoic acid) groups first reacted with each other via Glaser coupling, then subsequent dehydrogenative coupling of the acid moiety provided the corresponding polymeric bisacylperoxide in a domino reaction. Yang et al. [50] demonstrated that the dimerization and cyclotrimerization of acetyls could be used as a new way for on-surface phenyl formation, providing a promising approach for 2D conjugated covalent network construction. Recently, the catalytic dealkylation of ethers to alcohols on metal surfaces was reported, showing that the reactions can be well controlled by the annealing parameters [51]. Krüger et al. [52] presented the tetracene formation by the on-surface reduction of diepoxytetracenes. The mixture of *syn*/*anti*-isomers were deposited on Cu(111), and the thermal treatment turned them into tetracene in an efficient manner. The copper surface played an important role in both the deoxygenation and planarization processes.

Imines are important products in synthetic chemistry, which can be formed through the Schiff-base reaction between an aldehyde and an amine. The on-surface synthesis of imines was first performed by Weigelt and co-workers [23,24] on Au(111) in UHV, and 2D networks were achieved. Recently Jiang et al. [22] reported the on-surface synthesis of pyrene-fused pyrazaacene oligomers on Ag(111). They demonstrated that this reaction could be used as a useful tool to introduce nitrogen doping to covalently linked nanostructures. The Schiff-base cyclocondensation reaction of tetraketone and tetraamine precursors was triggered by thermal annealing on Ag(111). Au(111) and Cu(111) substrates were also tested to support this reaction, but the reactants desorbed from the Au(111) surface before the reaction took place, and decomposed on the Cu(111) surface during thermal treatment. The relationship between the stoichiometric proportions of reactants and the structure variations of the final products for on-surface Schiff-base condensation was studied by Gong et al. [21]. The rational production of identical discrete oligomers and high quality 2D covalently bonded networks was realized by controlling the stoichiometric proportions of 1,3,5-tris(4-formylphenyl)benzene and aromatic amines.

On-surface reactions based on boronic acid or metal–organic coordination

The cyclo-condensation of boronic acid was widely used to build 2D single-layer covalent organic frameworks on surfaces. The first example in UHV was reported by Zwaneveld et al. [25]. As a result, the synthesized networks were a mixture of pentagon, hexagon, and heptagon structures. In order to improve the structure regularity, thermodynamic equilibrium control and growth process control were carried out, this part of research works has been summarized and reviewed in reference [56].

Coordinative bonds, also called dative or semipolar bonds, are a type of 2-center, 2-electron covalent bonds in which both the shared electrons are supplied by one atom. Metal–organic coordinative interaction has been used to build 1D and 2D nanostructures on surfaces, known as surface confined metal–organic networks (SMONs). There are several excellent reviews summarized the various metal atoms and organic ligands involved in the synthesis of SMONs, comparing the different coordination motifs and the resulting structure topology diversity [54,55,75], which will not be elaborated here.

Techniques applied in the on-surface synthesis

Surface science techniques are widely used to study on-surface synthesis. Among them, scanning probe microscopy (SPM), including STM [76] and AFM [77,78], are the most popular methods due to their real-space atomic resolution. Nonlocal techniques, such as thermogravimetric analysis (TGA), X-ray photoelectron spectroscopy (XPS), ultraviolet photoelectron spectroscopy (UPS) and near edge X-ray absorption fine structure (NEXAFS), have also been used as complementary tools to reveal the on-surface reaction mechanisms. Theoretical methods, especially density functional theory (DFT) calculations, are used to simulate experimental results for detailed insights. In this part, we will introduce the principles and applications of the major techniques involved in the on-surface synthesis researches. New techniques, such as high pressure XPS and STM will also be briefly introduced as a future development direction.

Scanning probe microscopy (SPM)

Traditionally, the reaction products of organic synthesis are characterized by mass spectrum (MS) and nuclear magnetic resonance (NMR) and the reaction mechanisms are obtained by educated guess and empirical principles, which will be tested and revised over time to reveal the real bond breaking and formation process. The development of SPM providing atomic resolution in real space, makes the direct observation of single molecules and atoms at surfaces come true. With tip manipulation, molecules and atoms can be picked up from the surfaces and moved to the target positions to build complex constructions. Spectroscopy characterizations such as scanning tunneling spectroscopy (STS) can provide information about the material electronic, spintronic and optical properties with sub-molecular resolution. STM and STS have become the most powerful tools to examine on-surface reactions. They are widely used to directly analyze chemical structures and characterize properties of the reactants, intermediate products and final outcomes at the atomic scale, providing plenty of information about the reaction mechanisms and various control pathways to get designed architectures. However, the operation principles of STM and STS are based on detecting the local electronic density of states, therefore the image contrasts of molecules are not directly related to their chemical structures and the resolution is almost impossible to reach the chemical bond distinguishable level. Noncontact atomic force microscopy (nc-AFM) combined with a tuning fork based force sensor in the q-Plus configuration [79] has recently been used to investigate the on-surface reactions. Nc-AFM is a more recent technique which can provide 'wire-frame' chemical structures of molecules and even different chemical bond orders in a nondestructive way, mostly with the help of a CO-functionalized AFM tip currently.

In 2013, de Oteyza et al. [11] pioneered in applying nc-AFM to investigate on-surface reactions. The detailed internal bond transformations of the complex cyclization processes of oligo-(phenylene-1,2-ethynylenes) on Ag(111) was clearly revealed by high resolution nc-AFM images (shown in Fig. 7a). The reaction process was not directly followed by SPM like Hla et al. [62] did, but the surfaces were investigated after thermal treatment and different molecular species were searched out. The studies of using this technique to explore on-surface reactions bloomed since then. Pavliček et al. [80] succeeded in generating individual polycyclic aryne molecules on an ultrathin insulating film at cryogenic temperature and direct imaging of its chemical structure with the help of nc-AFM, demonstrating the potential of applying this method to the analysis of short-lived reaction intermediates. Arynes stand for the intermediate states of arenes by dehydrogenation from two adjacent carbon atoms, have long been predicted but hard to characterize due to their extremely high reactivity and short lifetimes. The cumulene resonance structure was suggested as the dominate one from contrast related bond order analysis of nc-AFM images. The reactivity of arynes was preserved even at cryogenic temperature, providing important potential applications in on-surface synthesis. Kawai et al. [81] investigated the transformation process of a sequential three-step reactions of a hydrocarbon molecule on Cu(111) with nc-AFM. The structures of the initial precursor, the final product and two intermediate states were clearly shown in the high resolution nc-AFM images, demonstrating its ability of following molecular transformations with unprecedented details. Kocić et al. [82] applied nc-AFM to study the mechanism of on-surface aryl–aryl dehydrogenation coupling reaction and revealed the origin of the reaction regioselectivity. The high-resolution AFM images, unambiguously distinguishing pyrazine from pyridine moieties, showed that the *ortho*-hydrogen atoms of the pyrazine rings were preferentially activated compared with their pyridine equivalents. Liu et al. [83] reported the on-surface synthesis of 1D conjugated polymers containing pentagons, which were clearly observed by nc-AFM. Riss et al. [84] synthesized the 1D oligo-(E)-1,1′-bi(indenylidene) polymers by enediyne cyclization and the following radical polymerization. The precise chemical structures of the monomers and the oligomers were revealed by nc-AFM, while the electronic properties were characterized by STM/STS. Combining the advantages of these two techniques, the reaction process and the mechanism can be revealed with unprecedented insights. Nc-AFM is more suitable for the study of materials with planar structures. For three-dimensional architectures, tip manipulation can be applied to transform them into 2D structures for better imaging. Majzik et al. [85] succeeded in the on-surface synthesis of a naphthodiazaborinine molecule, which represented a non-planar structure which could not be clearly imaged by nc-AFM. To solve this problem, H atoms were removed by tip bias pulse and the molecule was transformed into a 2D structure which then could be identified by nc-AFM.

In SPM applications, the tip configuration can significantly influence the resolution and contrast mechanism of the obtained images. For nc-AFM with sub-molecular resolution, the probe tip is operated at very short distance from the analyzed subject, where the repulsive force is dominant. This requires a chemical inert tip to avoid displacing or picking up molecules from the surface. CO-functionalized tip has been widely used with a very controllable formation by picking up a single CO molecule from the surface [84,86,87]. But the contrast mechanism with the CO-functionalized tip is nontrivial. The flexibility of the CO-tip apex may cause image distortions such as contrast sharpening of the molecule bonds or bond elongation [88,89]. Intermolecular features of organic molecules which were once ascribed as intermolecular bonds were identified as 'fake' bonds caused by tip flexibility [90]. To solve this problem, single atom functionalized tips were developed. Cl, Br and Xe atoms were used to give high resolution images, but none of them were connected to the metallic tip by covalent bonding, thus suffering from lateral displacements and the potential artifacts during scanning [91]. Recently, Mönig et al. [92] developed a

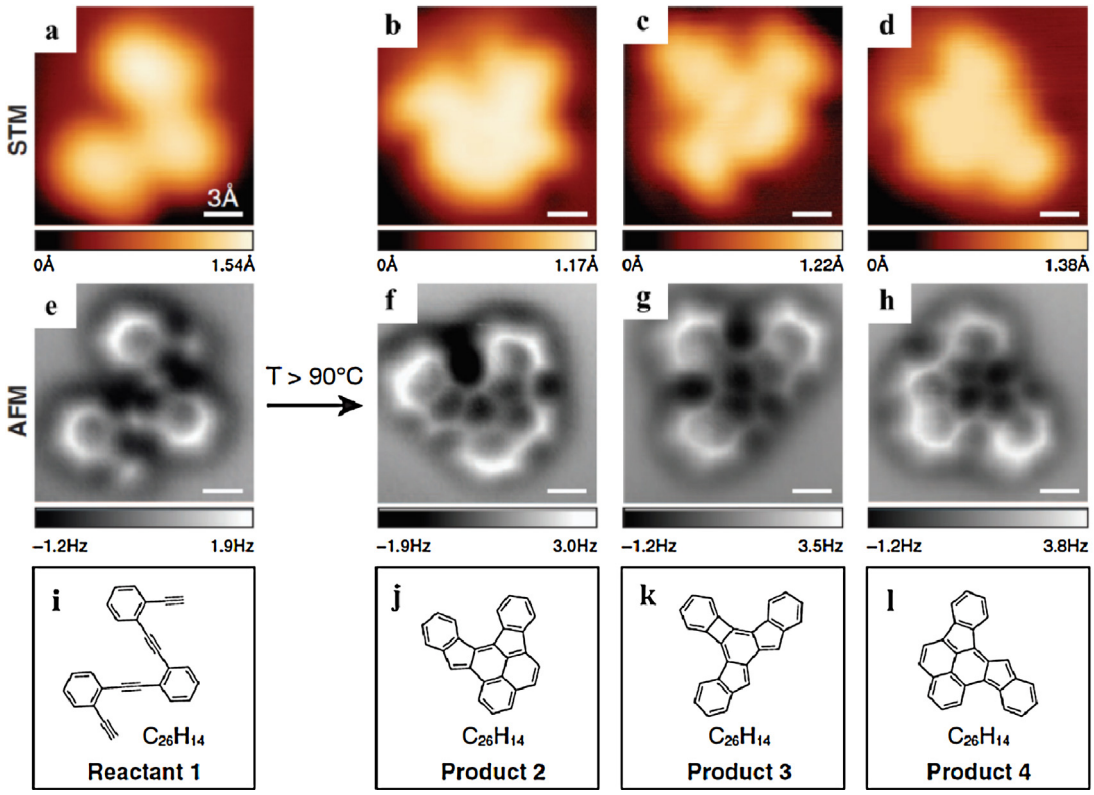

Fig. 7. STM images, nc-AFM images, and chemical structures for the reactants (a, e, i) and products (product 2: b, f, j; product 3: c, g, k; product 4: d, h, l) of an on-surface Bergman cyclization. Copyright© 2013, American Association for the Advancement of Science, reprinted with permission from Ref. [11].

new type of O-terminated tip by simply moving the pure Cu tip into the oxide domain by only a few angstroms on a partially oxidized Cu(110) surface. The chemical connection between the O apex and the Cu tip is covalent, offering high chemical and structural stability along with chemical inertness. They tested this new kind of tip by imaging an organic molecule, and by revealing its internal bond structures demonstrated that the lateral deflections of the terminal O atom were negligible (Fig. 8). This O-terminated Cu tip is a highly attractive probe solution for high resolution nc-AFM performance.

From STM to AFM, the spatial resolution of single molecules are getting higher and higher, but the chemical identification is still difficult, becoming a drawback for their further applications. Inelastic electron tunneling spectroscopy (IETS) and tip-enhanced Raman spectroscopy (TERS) may serve as their compensations. Their basic principles, technic issues, applications and recent advances have been reviewed before [93–96], which will, therefore, not be repeated here. Usually, it will take several minutes to get a typical STM or AFM image and the timescale of a dI/dV mapping may even extend to hours. In order to trace the rapid reaction process and to explore the reaction dynamics, ultrafast equipment will be needed. Recently, a low-temperature terahertz STM (THz-STM) was developed and applied to tracking a pentacene molecule by femtosecond orbital imaging [97]. Until now, none of these new techniques have been applied to the characterization of on-surface reaction processes, but may indicate a promising direction for the future development.

XPS technique

XPS, which is a surface-sensitive spectroscopic technique, offering information about the chemical and electronic states of the elements at the surface of a material within the first few nanometers, has been used to reveal the bond breaking and formation procedures. For example, the C 1s XPS spectrum of on-surface synthesized metalated carbyne chains showed two peaks corresponding to the unsaturated carbon atoms and the metal coordinated carbon atoms respectively, strongly supported the proposed $[—Cu—C—C—]_n$ structure [36]. Temperature dependent XPS spectra can depict the whole reaction process. XPS can not only show the bond transformation or the molecule desorption, but also reflect the substrate structure change induced by molecule adsorption and reaction. For example, the lifting and reappearance of the herringbone reconstruction were shown in the shifting of the C 1s spectrum for the Ullmann coupling and the dehydrogenation process of 4,4′-dibromo-p-terphenyl (DBTP) on Au(111). Compared with the on-surface reactions between DBBA molecules, XPS results showed that the Br atoms desorbed at much lower temperatures for DBTP, resulting in a much cleaner surface [98]. When carboxylic acid, ester, ether or acetyl groups are involved in on-surface reactions, it is difficult to distinguish whether the oxygen atoms are detached or not based on STM images only. The C 1s and O 1s XPS spectrum can clearly show the bond connection status. For example, for the dealkylation of ethers on Au(111) reported by Yang et al. [51], the strong O 1s XPS signal after thermal treatment suggested that the O atoms remained on the benzene side after reaction. The transformation of hydroxyl groups to carbonyl groups and eventually deoxygenation processes of 1,3,5-tris(4-hydroxyphenyl)benzene (THPB) on Au(111) and Ag(111) reported by Li et al. [16] were demonstrated by O 1s and C 1s spectra. XPS results also showed that the reaction happened at lower temperatures on Ag(111) compared with Au(111). Held et al. [49] reported the domino reactions occurring between biscarboxylic acids, and the bisacylperoxides formation were confirmed by the good correlation between the XPS data acquired from the on-surface synthesized polymers and the one from the ex situ prepared bis(2-naphthoyl) peroxide reference compounds. Wurster et al.

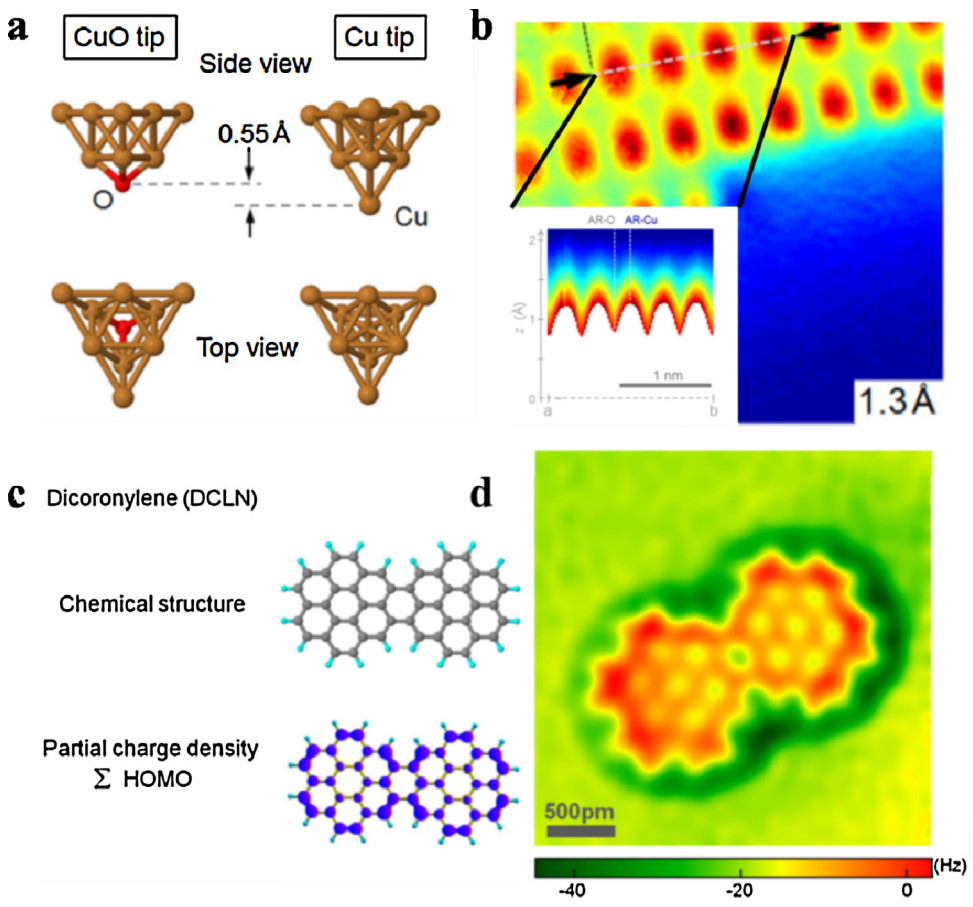

Fig. 8. Covalently linked O-terminated Cu nc-AFM tip and its applications in imaging organic molecules. (a) Structure model of a CuO tip and a Cu tip. (b) Horizontal force cut of the 3D nc-AFM data of a CuO surface with a CuO tip. Inset: the corresponding vertical force cut. (c) Chemical structural model and partial charge density of the occupied molecular orbitals (HOMO + HOMO1 + HOMO2) of DCLN. (d) Constant-height frequency shift image of a single DCLN on Cu(110) with a CuO tip. Copyright© 2016, American Chemical Society, reprinted with permission from Ref. [92].

[30] prepared a bimetallic coordinated catalyst through on-surface synthesis, and XPS was applied to check the chemical integrity and the oxidation state of the catalyst after catalytic reaction.

Density functional theory (DFT) stimulations

DFT, a quantum mechanical computational method, is an inevitable powerful tool for on-surface reaction studies. It is widely used to calculate the electronic structures of molecules, substrates and synthesized nano-architectures, which can be used as basis to simulate STM and AFM images with other methods such as the Tersoff–Hamann approach. For example, in the research of the on-surface synthesis of 1D polymer chains through Bergman cyclization reported by Sun et al. [12], the heart-shaped STM images and the staggered chains with two columns of protrusions after annealing at ~400 K were assigned to the intact precursor molecules and the Bergman reaction produced polyphenylenes by comparing the STM results with the DFT simulated images, respectively (Fig. 2c).

Material properties measured by STS and other spectroscopy methods were compared with DFT simulations for a better understanding. Taking the on-surface synthesized graphene nanoribbons (GNRs) as an example, Cloke et al. [99] reported the on-surface synthesis of site-specific boron doped GNRs, the band structures were measured by dI/dV mapping and simulated by DFT. Both the experimental and theoretical local density of states (LDOS) maps proved a significant increase in the electronic structures of the GNRs by boron doping. The band structures of the width-modulated 7–13 GNRs synthesized by Chen et al. [100] were also tested by dI/dV mapping and proved to be similar to type I semiconductor heterojunction behavior. These results were supported by DFT calculations. The conductance [101] and the mechanical properties [102] of a single GNR were measured by lifting it from the surface with the STM or AFM tips, and the experimental conductance and sliding behavior were compared with the simulated results for a microscopic insight.

Reaction pathways and the relative activation energies were also calculated by DFT to gain further information about the reaction mechanisms, which have recently been reviewed by Björk [103].

High pressure surface-sensitive techniques

Important industrial catalytical processes such as Fischer–Tropsch synthesis and methane steam reforming are performed under high pressures and high temperatures, while the catalysts behave significantly different from the models studied by surface science at UHV conditions. The pressure and material gaps are great challenges for the understanding of the industrial heterogeneous catalytic processes, hampering the rational design of high efficient and highly selective catalysts. High pressure surface-sensitive techniques such as near ambient pressure XPS (NAP-XPS), high-pressure STM (HP-STM) and environmental transmission electron microscopy (ETEM) have been utilized to explore the structure and composition complexities of catalysts under working conditions during the past decades, as has been reviewed

by Tao et al. [104,105]. The development of the surface-sensitive techniques working at high pressures and high temperatures will dramatically accelerate the applications of on-surface synthesis in industry.

On-surface synthesized functional architectures

The development of nano-electronics, spintronics, photonics and catalysts requires the precision construction of multicomponent and multilevel nanostructures with high stability on all sorts of surfaces. The traditional organic synthesis can produce all sorts of products, but as the sizes of the desired structures grow bigger, the synthesis difficulty increases in an exponential way, and the accompanying purifying process could become unreachable. It will also be a great challenge to place these structures in a freely controllable manner onto the substrate surfaces for further applications. On-surface synthesis is a bottom-up strategy for building up covalently linked nanostructures, offering a clean, efficient and controllable way for the construction of advanced materials and molecular devices. 1D nanowires and 2D networks with organic or organometallic components were synthesized on various surfaces, which have already been mentioned in the above summary of reaction types and will not be discussed here again. Within this part, we would like to focus on the bottom-up formation of GNRs as an important example of on-surface synthesized novel functional architectures.

Graphene is a 2D atomic-thick honeycomb nanosheet of carbon, and as a Dirac material exhibiting a zero-effective charge carrier mass, it has many desirable properties such as ballistic charge transport, thus offering a great opportunity for the construction of high-performance graphene-based electronics. However, the lack of band gap severely limits its applications in semiconductor devices. By shrinking the dimensions of nanosheets to nanoribbons, the electronic band gap can be opened and the materials will show semiconductor properties originating from the quantum confinement and edge effects. Several methods have been explored to get GNRs, such as chemical [106,107] or sonochemical [108] synthesis, lithographic method [109,110] and unzipping carbon nanotubes [111], but none of those strategies could control the width and edge structures of GNRs with atomic precision.

In 2010, Cai et al. [42] first applied on-surface Ullmann coupling and subsequent cyclodehydrogenation reactions of 10,10′-dibromo-9,9′-bianthryl (DBBA) molecules to build armchair GNRs, demonstrating the possibility of finely controlling the topology, width and edge periphery of GNRs by the design of the molecule precursors (Fig. 9a). The following work of Talirz et al. [112] discussed the termini of the synthesized armchair GNRs, showing that it was passivated by hydrogen, indicating that the length of the nanoribbon should be able to be controlled by the pressure of H_2 during polymerization. Linden et al. [113] reported the bottom-up synthesis of the spatially well-aligned straight armchair GNRs and chevron-type GNRs on a stepped Au(788) surface, allowing a 1D orientation of the resulting GNRs. The direct and inverse angle resolved photoemission spectroscopy (ARPES) results of the occupied and unoccupied states of the different types of GNRs clearly proved the existence of large tunable electronic band gaps.

From then on, the researches of on-surface synthesis of GNRs were blooming. Different types of reactions involving a great diversity of molecule precursors were exploded to get GNRs with fine-tuned width and edge structures. Basagni et al. [98] showed that the lateral dehydrogenation and C—C coupling could be used to get GNRs from 1D polymer chains, proposed a new way for the fabrication of GNRs. To further narrow the width of the synthesized GNRs, Kimouche et al. [114] used dibromoperylene as precursors and succeeded in the synthesis of $n = 5$ GNRs on Au(111). STM results showed that it had metallic behavior with a very small bandgap, which was not strongly affected by defects. But similar 5-AGNR synthesized by Zhang et al. [115] by using 1,4,5,8-tetrabromonaphthalene molecules as the precursors on Au(111) showed an unexpected large bandgap, which was explained by the hybridization with the surface states. Another milestone of the on-surface synthesis of GNRs is the fabrication of GNRs with zigzag edges which were predicted to have great potential in the application of spintronics. With specifically designed precursors, Ruffieux et al. [116] reported the on-surface synthesis of GNRs with atomically precise zigzag edges (Fig. 9b). The edge localized states showed great energy splitting. Recently Sakaguchi et al. [117] designed a "Z-bar-linkage" precursor which exhibits geometric flexibility to adopt an optimized conformation on Au(111). Acene-type GNRs with 1.45 nm width were synthesized through a new "conformation-controlled surface catalysis" method.

On-surface synthesis has also been explored in the construction of heterojuctions and doped GNRs. By changing the structures of the precursors, Chen et al. [118] succeed in the synthesis of $n = 13$ armchair nanoribbons, which showed a smaller band gap compared with the $n = 7$ armchair GNRs. Then by fusing segments made from these two different kinds of building blocks, they obtained width-modulated armchair GNR heterojunctions on surface, demonstrating bandgap engineering at the molecule scale [100]. By introducing N-substituted precursors, N-doped GNRs were synthesized on Au(111) by Cai et al. [119], and by further combining pristine hydrocarbon precursors with their N-doped equivalents, partially doped GNR heterostructures were fabricated and showed similar behavior as traditional p–n junctions, bearing a high potential in the applications of photovoltaics and electronics. Cloke et al. [99] introduced B atoms into the backbones of the DBBA molecules, and the STM images of the fully cyclized B-doped GNRs showed a period corresponding to the positions of the doped B atoms, consistent with the conjugation between the empty p-orbital of B atoms and the extended π-system of DBBA molecule backbones. Apart from N and B doping, on-surface synthesis has also been applied to the decoration of graphene edges with other molecules to build multicomponent systems. He et al. [120] reported the dehydrogenative coupling of porphine molecules to graphene edges. STM and AFM were applied to explore the bond motifs and the electronic features, demonstrating that the reactions happened at the pyrrole rings of porphines. More interestingly, the graphene-anchored tetrapyrrole macrocycles kept the ability of metalation with silver atoms and further axial ligation with adducts such as CO molecules, which demonstrated that on-surface synthesis was capable of complex multifunctional nanostructure construction.

Potential applications

As a newly-developed research area, it is intriguing to see that several real applications of on-surface synthesized nanomaterials were explored.

Carbon capture

Carbon dioxide (CO_2) is a greenhouse gas whose concentration has been increased in the atmosphere by the extensive usage of fossil fuel and industrial processes, which will result in severe environmental problems such as global warming and ocean acidification. Carbon capture and storage are technologies that can be used to reduce CO_2 emissions from human activities, preventing them from entering the atmosphere. Further conversion of CO_2 into high-energy density compounds will fundamentally solve the

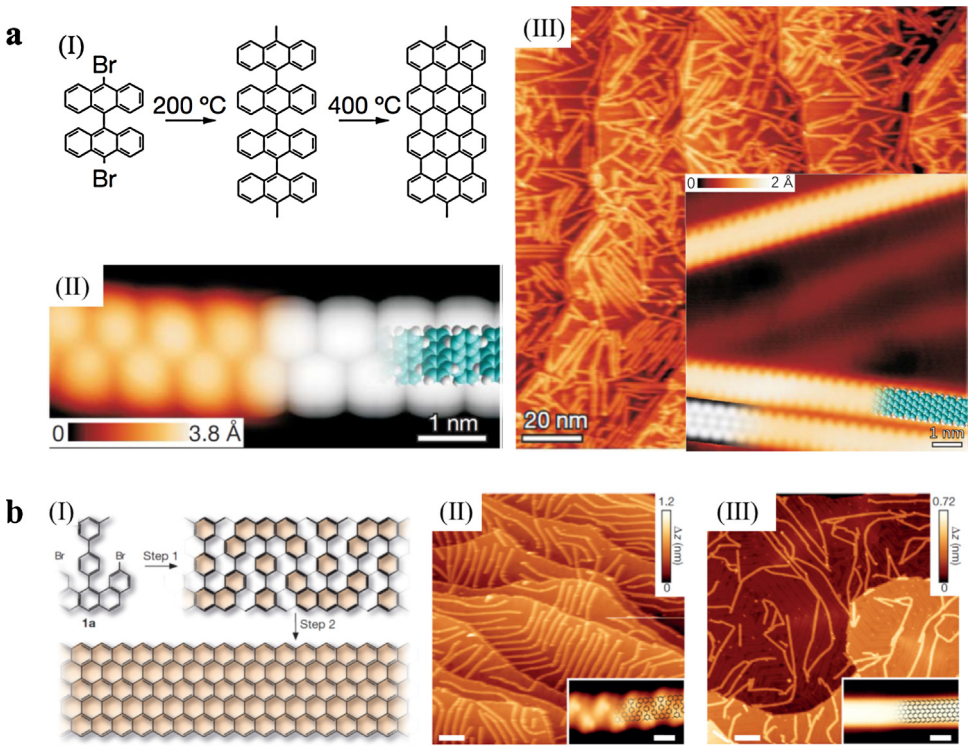

Fig. 9. On-surface synthesized armchair and zigzag GNRs. (a) Bottom-up fabrication of armchair GNRs. (I) Schematic illustration of the synthesis strategy of GNRs with armchair edges. (II) STM image of a polyanthrylene chain after annealing at 200 °C. DFT-based simulation of the STM image shown in the right with partially superimposed structure model of the polymer. (III) STM image of the straight $N = 7$ GNRs after cyclodehydrogenation at 400 °C. Inset: a high-resolution STM image with partly superimposed molecular model and a DFT-based STM simulation (greyscale image). Copyright© 2010, Nature Publishing Group, reprinted with permission from Ref. [42]. (b) Bottom-up synthesis of zigzag GNRs. (I) Schematic illustration of the synthetic strategy of GNRs with zigzag edges. (II) Large scale (scale bar, 20 nm) and high-resolution (inset, scale bar 1 nm) STM images of the polymers after dehalogenation. (III) Large scale (scale bar, 20 nm) and high-resolution (inset, scale bar 1 nm) STM images of the GNRs with zigzag edges. Copyright© 2016, Nature Publishing Group, reprinted with permission from Ref. [116].

problem between the global energy demand and the depletion of fossil fuel.

The first step of CO_2 utilization is the capturing of CO_2 at its source which requires the separation of CO_2 from other gases produced by industrial processes. On-surface synthesized 1D and 2D metal–organic nanostructures were reported having CO_2 adsorption abilities and the microscopic mechanisms were provided by surface-sensitive techniques. The 1D metal–organic chains were synthesized by 1,4-phenylene diisocyanide (PDI) units coordinating with substrate Au adatoms. CO_2 adsorption on Au-PDI chains supported on gold surfaces at 90 K could change the initially uniformly dispersed chains into close packed bundles, self-catalyzing their own capture. This process was reversible. At high temperatures, the adsorbed CO_2 molecules could be released and the metal–organic chains would return to their original forms [121] (Fig. 10a). While at lower temperatures, such as liquid helium temperature, the observed CO_2-organometalic chains interaction was different. $CO_2^{\delta-}$ species formed by coordinating with Au adatoms would seed the subsequent physisorption of CO_2 molecules. XPS and infrared reflection absorption spectroscopy (IRAS) results confirmed the charge transfer from the substrate to adsorbed CO_2 molecules. STM images clearly showed the progressive CO_2 physical absorption process from dimers to 1D chains, 2D islands and eventually a monolayer [122]. The interaction of CO_2 with a 2D Fe-carboxylate metal–organic network was reported to result in the collapse of the network structure. STM results combined with DFT calculations revealed the binding motifs of CO_2 with Fe adatoms and the carboxylate ligands [123]. The microscopic understanding of the CO_2 capture mechanism is vitally important for the rational design of CO_2 enrichment materials with high efficiency and selectivity.

Quantum box

On-surface synthesized 2D nanoporous networks can be used as quantum boxes for hosting other atoms or molecules to form well-defined superlattice structures. For example, Pivetta and co-workers [124] succeeded in the formation of Fe atoms and clusters superlattice in a dicarbonitrile pentaphenyl–Cu coordination honeycomb network (Fig. 10b). Nowakowska et al. [125] examined the atom-by-atom condensation process of Xe atoms within a highly-ordered Cu-coordinated, triply dehydrogenated 4,9-diaminoperylene quinone-3,10-diimine (3deh-DPDI) porous network. The subtle interplay between the competing directional and nondirectional forces was revealed.

As an example of the molecules hosted in 2D quantum boxes, Fe-carboxylate coordinated networks were used to accommodate C_{60} guest molecules on a Cu(100) surface. The pore sizes and chemical functionalities of Fe-carboxylate networks could be fine-tuned by the structures of the linker molecules and thermal treatments; meanwhile the host–guest interactions would be varied accordingly [126]. Caging into a 2D quantum box would change the chemical environment of the guest molecules, which may result in the formation of novel structures with exotic properties. Supramolecular noncovalent-linked dynamers were constructed by hosting *para*-sexiphenyl-dicarbonitrile (NC-Ph_6-CN) trimers into a Co-NC-Ph_6-CN coordinated network with regular hexagonal 24 nm^2-area pores. The concerted, chirality-preserved rotary motions of the caged dynamers were observed and analyzed by temperature-controlled STM [127]. The molecular Kondo effects of Co-tetra-pyridyl-porphyrin (Co-TPyP) molecules could be switched by different supramolecular environments. When Co-TPyP were trapped inside 2D nanoporous networks on Cu(111) or Au(111),

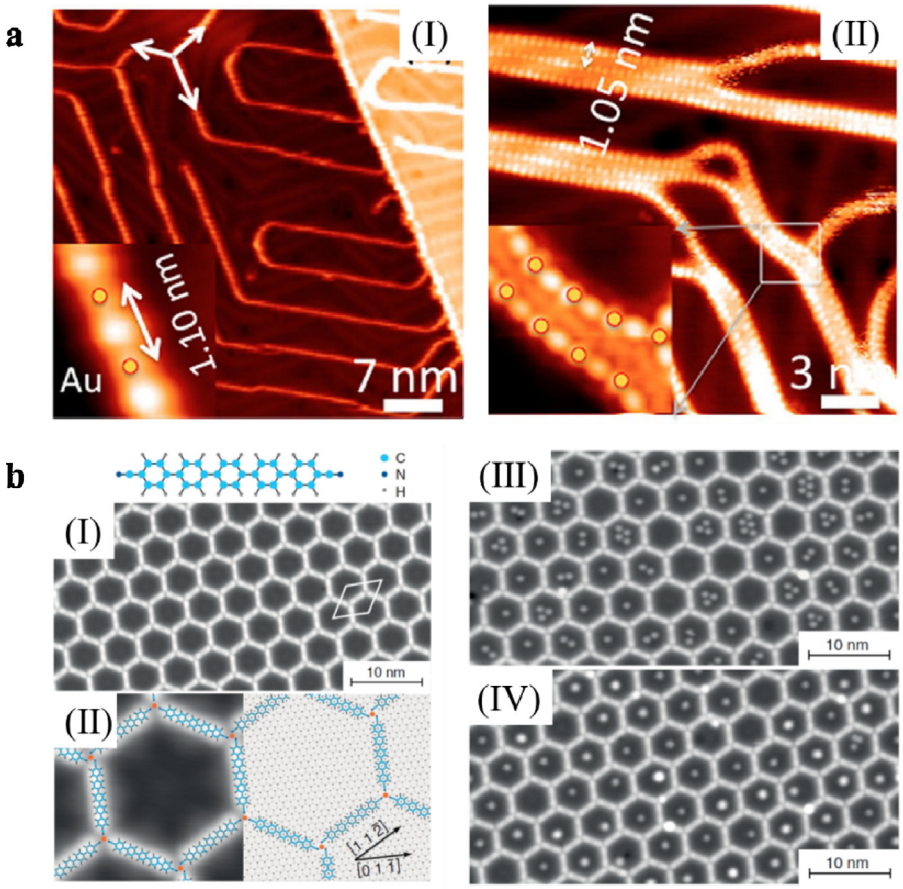

Fig. 10. Applications of metal–organic coordinated nanostructures in carbon capture and quantum box. (a) Self-catalyzed CO_2 capture by 1D metal–organic chains. (I) STM image of dispersed Au-PDI chains on Au(111). Inset: a high-resolution STM image shown the Au adatoms and PDI units. (II) STM images of a sub-monolayer Au-PDI chains after CO_2 dosing at 90 K. Inset: CO_2 molecules captured by a pair of Au-PDI chains. Copyright© 2014, American Chemical Society, reprinted with permission from Ref. [121]. (b) Formation of Fe atoms and clusters in a metal–organic quantum box network. (I) Large scale STM image of $(NC\text{-}Ph_3\text{-}CN)_3Cu_2$ honeycomb network. (II) High-resolution STM image superimposed with the structure model. (III) STM images of Fe adatoms in the template cavities (IV) STM images of Fe clusters after annealing. Copyright© 2013 American Physical Society, reprinted with permission from Ref. [124].

the Kondo effect associated with the Co center could be switched on and off and the Kondo temperature could be modulated due to the different adsorption heights [128].

Single molecular conductance

The single molecular conductance information is of vital importance for the development of molecular circuits where the molecules are involved as electronic communication wires and functional units. Statistical methods [129] such as break junctions are involved to measure molecular conductance, but precise single molecular charge transport corresponding to the chemical environment is unreachable for these methods. With the help of STM tip manipulation, the on-surface synthesized polymer wires or GNRs can be lifted from the surfaces and the relationship between the conductance and the molecular length can be determined.

The pioneer work of Lafferentz et al. [1] tested the length-dependent conductance of a single polyfluorene wire synthesized by on-surface Ullmann coupling, demonstrated that the conductance decayed as the molecular wire was pulled up from the Au(111) surface. A characteristic step-like modulation in the current versus distance curves related to the step-by-step detaching of the building blocks were observed and analyzed (Fig. 11a). The conductance of a single on-surface synthesized GNR was also examined [101], showing that both the atomic structure and the electronic state would affect the conductance. The high conductance was reached at the delocalized electronic states of the nanoribbon. A planar geometry was demonstrated to be important, because molecular bending would reduce the charge transport. The edge structures were expected to be able to control the conductance of the GNRs. Zigzag edges would show pseudo-ballistic characteristic, while armchair edges were preferred in tunneling regime. To get high conductance, a small highest occupied molecular orbital (HOMO) and lowest unoccupied molecular orbital (LUMO) gap will be preferred. By introducing alternative oligothiophene donors and benzobis(1,2,5-thiadiazole) acceptors as building blocks, the on-surface synthesized polymers showed a high conductance without sacrificing the structure flexibility and the band gap. More importantly, electronic delocalization was proved to be not necessary for a highly effective charge transport [130]. Recently, a length-independent conducting behavior was reported for the on-surface synthesized conjugated polyporphyrin wires with a length of over 10 nm [131]. First-principle calculations showed that the measured conductance was channeled by resonant transport via the delocalized LUMO levels of the molecules. Mechanic force was reported to have an influence on the molecular conductance. An abrupt conductance increase during the pulling process of a polythiophene wire from the Au(111) surface was measured and associated with the stress relaxation [132]. For the construction of complex nanostructures, nonsymmetrical molecule nodes were synthesized and

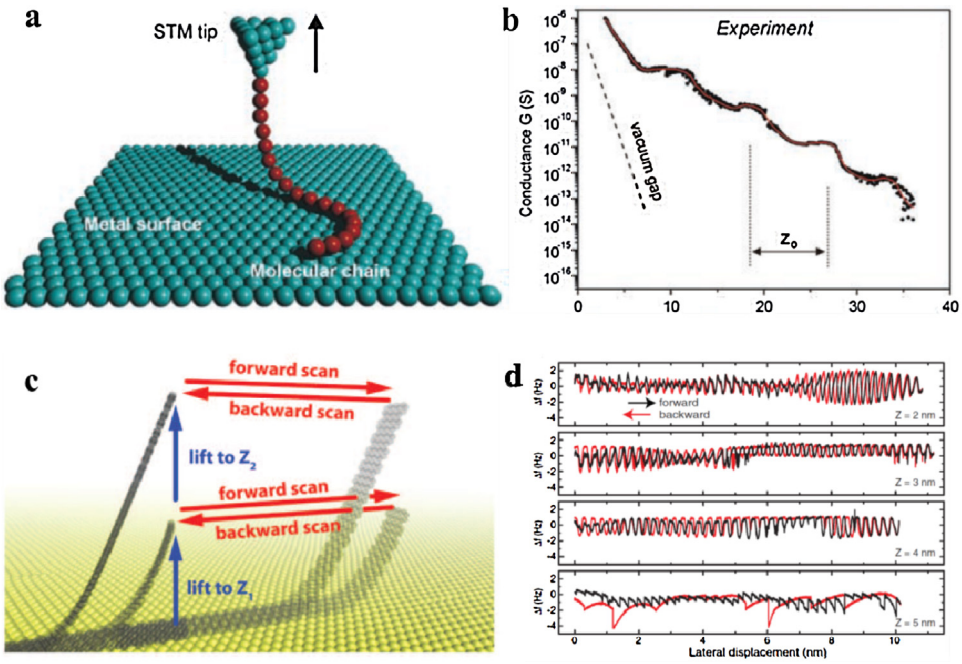

Fig. 11. Tip manipulation application in single molecular property measurement. (a) Schematic illustration of lifting a single molecular chain from the surface with a STM tip. (b) Conductance as a function of molecular length. Copyright© 2009, American Association for the Advancement of Science, reprinted with permission from Ref. [1]. (c) Schematic illustration of the lateral manipulation of a GNR on Au(111) with an AFM tip. (d) Frequency shifts as a function of pulling heights. Copyright© 2016, American Association for the Advancement of Science, reprinted with permission from Ref. [102].

utilized in on-surface reactions. A nonsymmetrical Y-shaped polymer was built from bottom up and the measured conductance showed subtle differences between different transport channels [6].

Single molecular mechanical property

When low temperature AFM was applied to pull a single molecular wire or GNR from the surfaces, the mechanical properties can be measured accordingly. Kawai and co-workers tested the atomic-level mechanics of a single on-surface synthesized polyfluorene wire [133] and GNR [102]. For the polyfluorene chains, the periodicity and magnitude of the measured force gradient were related to the step-by-step detachment force and the desorption energy of an individual fluorene repeat unit. For the GNRs on gold surfaces, superlubricity was discovered and studied. The importance of the ribbon size and elasticity, the influence of the surface reconstruction were unraveled by a combined experimental and computational approach (Fig. 11b).

Luminescence

When an emitting molecular center is connected in the middle of the on-surface synthesized polymer wire and pulled up, thus becoming decoupled from the metal surface, the tunneling electron induced single molecular luminescence could be measured by a special designed STM [134]. An ultranarrow-line emission associated to the fluorescence of the porphyrin molecular emitter was discovered. The linewidth can be controlled by step-by-step detaching of the emitting molecular center from the surface. Several low-intensity vibronic peaks provided a fingerprint of the molecular emitter. Localized surface plasmons were demonstrated to be important for the molecular excitation and emission (Fig. 11c).

Magnetic polymers (for spintronic devices)

Molecular based spintronic devices are important components of future information technologies such as data storage and quantum computers, which can be formed by covalently-linked magnetic molecules. DiLullo et al. [135] reported the construction of 1D multi-spin center macromolecules by the Ullmann coupling of Co-(5,5′-Br_2–Salophen) on Au(111). Separate Kondo regions of the independent molecular building blocks were observed and the antiferromagnetic coupling between them was revealed by DFT calculations. Also by Ullmann coupling of Co-Salophene based precursors, an all-spin molecular device was reported by Bazarnik et al. [29]. Compared with their atomic counterparts, the operation temperature of the devices was enhanced by the strong covalent bond.

Field effect transistors (FETs)

Combined with the transfer technique, the on-surface synthesized materials can be peeled off and transferred to the dielectric surfaces to make FETs by nano-fabrication. Sakaguchi and co-workers [117] reported the FET constructions based on the on-surface synthesized homochiral GNRs. The FETs exhibited ambipolar semiconductor properties with a hole mobility of 0.26 $cm^2 V^{-1} s^{-1}$ and an on/off ratio of 88. Chen et al. [136] extended the on-surface synthesis of GNRs to chemical vapor deposition (CVD) under ambient-pressure conditions, and large-scale homogenous GNRs were obtained and transferred to fabricate FETs which exhibited a high current on/off ratio of up to 6000. N-doped and N,S-co-doped GNRs as well as their heterojunctions were also synthesized and characterized by Raman, mass spectrometry, high resolution electron energy loss spectroscopy (HREELS), XPS, and STM. This transformation method successfully overcomes the drawback of the substrate differences between the on-surface synthesis and device fabrications, paving way for the real electronic

device applications based on on-surface synthesized nanomaterials.

Catalytical application

On-surface synthesis can also be applied to the rational design of new efficient catalysts. The unsaturated metal centers of the on-surface synthesized metal–organic nanostructures have drawn plenty of research attentions for their potential applications in catalysis. For example, the di-iron centers of Fe-terephthalic acid (TPA) coordination networks were used to mimic the non-heme enzymes for oxygen dissociation [137]. This part of work have been reviewed by Gutzler et al. [55]. Recently, another example provided by Wurster et al. [30] demonstrated that the metal–organic networks containing single iron and cobalt atoms can significantly increase the catalytic activity of the oxygen evolution reaction (OER) in a nonlinear way.

To bridge the material and pressure gap between the surface science studied model catalysts and the heterogeneous catalysts applied in industrial processes, high pressure and high temperature surface-sensitive techniques such as NAP-XPS and HP-STM are developed and used to study catalytical processes. Several reviews have summarized the development milestones in this area [104,105]. Most recently, in situ Fischer–Tropsch synthesis on cobalt surfaces was studied by Navarro et al. [138] with the help of a specially designed STM operating under reaction conditions. The self-assembly of long linear hydrocarbon products with 14 or 15 carbon atom length was observed on the terraces of the cobalt surface after 40 min of reaction at $221 \pm 10\,^{\circ}C$ under a flow of mixed hydrogen and argon gas ($P_{H_2} : P_{Ar} = 1 : 4$) with a total pressure of 4 bar. A simple model was proposed to explain the observed phenomena.

Perspectives and conclusion

In this review, we summarized all the on-surface reaction types by using a systematic scheme of different chemical bonding states of carbon (SP^0-C, SP^1-C, SP^2-C, SP^3-C, C—O, C═O, etc.). We discussed new techniques used in the study of on-surface reactions, and beyond the widely used STM techniques, the development of nc-AFM and some new techniques such as TERS and HP-STM which carry great potentials. The on-surface reactions discussed here have been used to build 1D and 2D covalently linked nanostructures on surfaces. Taking GNRs as an example, we showed the superior strength of this method in controlling the structures with atomic precision. The potential applications of the on-surface synthesized nanomaterials have been explored, ranging from molecular devices to catalysts, which were also discussed here.

Currently, only a small part of traditional organic synthesis which has developed hundreds of chemical reactions during the past centuries has been realized on surfaces. Thus, the future development of on-surface synthesis will be continuously devoted to the realization of new reaction types with increasing complexity. With the help of the molecular precursor design and the appropriate choice of the substrate, novel reaction types will be identified which will work particularly well or even exclusively on surfaces, and which will make use of cooperative effects (catalysis), taking advantage of the presence of a free surface or a buried interface, and surface induced chirality. Dimensional constraints, for example, posed by nanostructured surfaces allowing regioselective control of the reaction processes will be used as well. Inherent to vacuum techniques is the possibility of a well controllable surface quality and sample temperature thus allowing to stabilize short-living transitional states at low temperatures to study chemical reaction mechanism in detail, molecule by molecule. In future, we will progressively see the combination of scanning probe techniques providing highest special resolution with highest temporal resolution based on nanophotonic approaches to understand also the dynamic behavior of a reaction better. In addition, chemical sensitive, nondestructive techniques will be added to identify the chemical nature of molecular systems locally.

With the improvement of these techniques and the closer collaboration of chemists, physicists and material scientists, including experiment and theory, more complex multilevel bottom-up structures and stimuli responsive systems beyond two dimensions will come into practical range. Bio-inspired concepts may then come more and more into play to generate soft nanosystems with emergent properties, which will go far beyond nowadays chemical approaches and the limited properties of the chemical units building them up. The combination of weak and strong interactions will be needed to fulfill this target. We find ample blueprints in biology. On a more remote timescale, many new soft materials and unprecedented devices including, for example, thermodynamically open systems with self-repairing capabilities can be foreseen, which will not just replace the existing technologies based on silicon or metallic alloys, but will find new technological niches based on their tailored mechanical and opto-electronic properties as well as biocompatibility. To reach these goals, differing bottom-up and top-down strategies as well as template assisted techniques will have to be combined in a smart way for getting novel advanced materials.

Acknowledgements

We thank the Deutsche Forschungsgemeinschaft, TRR 61 and SFB 858, for financial support, as well as the National Natural Science Foundation of China (21673118), Natural Science Foundation of the Higher Education Institutions of Jiangsu Province, China (16KJB150018) and the China Scholarship Council (201608320070).

References

[1] L. Lafferentz, F. Ample, H. Yu, S. Hecht, C. Joachim, L. Grill, Science 323 (2009) 1193–1197.
[2] L. Grill, M. Dyer, L. Lafferentz, M. Persson, M.V. Peters, S. Hecht, Nat. Nanotechnol. 2 (2007) 687–691.
[3] L. Lafferentz, V. Eberhardt, C. Dri, C. Africh, G. Comelli, F. Esch, S. Hecht, L. Grill, Nat. Chem. 4 (2012) 215–220.
[4] W. Wang, X. Shi, S. Wang, M.A. Van Hove, N. Lin, J. Am. Chem. Soc. 133 (2011) 13264–13267.
[5] M. Bieri, M.-T. Nguyen, O. Gröning, J. Cai, M. Treier, K. Aït-Mansour, P. Ruffieux, C.A. Pignedoli, D. Passerone, M. Kastler, K. Müllen, R. Fasel, J. Am. Chem. Soc. 132 (2010) 16669–16676.
[6] C. Nacci, A. Viertel, S. Hecht, L. Grill, Angew. Chem. Int. Ed. 55 (2016) 13724–13728.
[7] Q. Fan, C. Wang, Y. Han, J. Zhu, W. Hieringer, J. Kuttner, G. Hilt, J.M. Gottfried, Angew. Chem. Int. Ed. 52 (2013) 4668–4672.
[8] Y.-Q. Zhang, N. Kepčija, M. Kleinschrodt, K. Diller, S. Fischer, A.C. Papageorgiou, F. Allegretti, J. Björk, S. Klyatskaya, F. Klappenberger, M. Ruben, J.V. Barth, Nat. Commun. 3 (2012) 1286.
[9] H.-Y. Gao, H. Wagner, D. Zhong, J.-H. Franke, A. Studer, H. Fuchs, Angew. Chem. Int. Ed. 52 (2013) 4024–4028.
[10] B. Cirera, Y.-Q. Zhang, J. Björk, S. Klyatskaya, Z. Chen, M. Ruben, J.V. Barth, F. Klappenberger, Nano Lett. 14 (2014) 1891–1897.
[11] D.G. de Oteyza, P. Gorman, Y.-C. Chen, S. Wickenburg, A. Riss, D.J. Mowbray, G. Etkin, Z. Pedramrazi, H.-Z. Tsai, A. Rubio, M.F. Crommie, F.R. Fischer, Science 340 (2013) 1434–1437.
[12] Q. Sun, C. Zhang, Z. Li, H. Kong, Q. Tan, A. Hu, W. Xu, J. Am. Chem. Soc. 135 (2013) 8448–8451.
[13] K. Amsharov, N. Abdurakhmanova, S. Stepanow, S. Rauschenbach, M. Jansen, K. Kern, Angew. Chem. Int. Ed. 49 (2010) 9392–9396.
[14] K.T. Rim, M. Siaj, S. Xiao, M. Myers, V.D. Carpentier, L. Liu, C. Su, M.L. Steigerwald, M.S. Hybertsen, P.H. McBreen, G.W. Flynn, C. Nuckolls, Angew. Chem. Int. Ed. 46 (2007) 7891–7895.
[15] A. Floris, S. Haq, M. In't Veld, D.B. Amabilino, R. Raval, L. Kantorovich, J. Am. Chem. Soc. 138 (2016) 5837–5847.
[16] Q. Li, B. Yang, H. Lin, N. Aghdassi, K. Miao, J. Zhang, H. Zhang, Y. Li, S. Duhm, J. Fan, L. Chi, J. Am. Chem. Soc. 138 (2016) 2809–2814.

[17] A. Wiengarten, K. Seufert, W. Auwärter, D. Ecija, K. Diller, F. Allegretti, F. Bischoff, S. Fischer, D.A. Duncan, A.C. Papageorgiou, F. Klappenberger, R.G. Acres, T.H. Ngo, J.V. Barth, J. Am. Chem. Soc. 136 (2014) 9346–9354.
[18] M. Treier, C.A. Pignedoli, T. Laino, R. Rieger, K. Müllen, D. Passerone, R. Fasel, Nat. Chem. 3 (2011) 61–67.
[19] G. Otero, G. Biddau, C. Sanchez-Sanchez, R. Caillard, M.F. Lopez, C. Rogero, F.J. Palomares, N. Cabello, M.A. Basanta, J. Ortega, J. Mendez, A.M. Echavarren, R. Perez, B. Gomez-Lor, J.A. Martin-Gago, Nature 454 (2008) 865–868.
[20] A.C. Aragonès, N.L. Haworth, N. Darwish, S. Ciampi, N.J. Bloomfield, G.G. Wallace, I. Diez-Perez, M.L. Coote, Nature 531 (2016) 88–91.
[21] Z. Gong, B. Yang, H. Lin, Y. Tang, Z. Tang, J. Zhang, H. Zhang, Y. Li, Y. Xie, Q. Li, L. Chi, ACS Nano 10 (2016) 4228–4235.
[22] L. Jiang, A.C. Papageorgiou, S.C. Oh, Ö. Sağlam, J. Reichert, D.A. Duncan, Y.-Q. Zhang, F. Klappenberger, Y. Guo, F. Allegretti, S. More, R. Bhosale, A. Mateo-Alonso, J.V. Barth, ACS Nano 10 (2016) 1033–1041.
[23] S. Weigelt, C. Busse, C. Bombis, M.M. Knudsen, K.V. Gothelf, E. Lægsgaard, F. Besenbacher, T.R. Linderoth, Angew. Chem. Int. Ed. 47 (2008) 4406–4410.
[24] S. Weigelt, C. Busse, C. Bombis, M.M. Knudsen, K.V. Gothelf, T. Strunskus, C. Wöll, M. Dahlbom, B. Hammer, E. Lægsgaard, F. Besenbacher, T.R. Linderoth, Angew. Chem. Int. Ed. 46 (2007) 9227–9230.
[25] N.A.A. Zwaneveld, R. Pawlak, M. Abel, D. Catalin, D. Gigmes, D. Bertin, L. Porte, J. Am. Chem. Soc. 130 (2008) 6678–6679.
[26] X.-H. Liu, C.-Z. Guan, S.-Y. Ding, W. Wang, H.-J. Yan, D. Wang, L.-J. Wan, J. Am. Chem. Soc. 135 (2013) 10470–10474.
[27] J.F. Dienstmaier, D.D. Medina, M. Dogru, P. Knochel, T. Bein, W.M. Heckl, M. Lackinger, ACS Nano 6 (2012) 7234–7242.
[28] J.F. Dienstmaier, A.M. Gigler, A.J. Goetz, P. Knochel, T. Bein, A. Lyapin, S. Reichlmaier, W.M. Heckl, M. Lackinger, ACS Nano 5 (2011) 9737–9745.
[29] M. Bazarnik, B. Bugenhagen, M. Elsebach, E. Sierda, A. Frank, M.H. Prosenc, R. Wiesendanger, Nano Lett. 16 (2016) 577–582.
[30] B. Wurster, D. Grumelli, D. Hötger, R. Gutzler, K. Kern, J. Am. Chem. Soc. 138 (2016) 3623–3626.
[31] M. Matena, T. Riehm, M. Stöhr, T.A. Jung, L.H. Gade, Angew. Chem. Int. Ed. 47 (2008) 2414–2417.
[32] G. Wang, A. Rühling, S. Amirjalayer, M. Knor, J.B. Ernst, C. Richter, H.-J. Gao, A. Timmer, H.-Y. Gao, N.L. Doltsinis, F. Glorius, H. Fuchs, Nat. Chem. 9 (2017) 152–156.
[33] C.M. Crudden, J.H. Horton, I.I. Ebralidze, O.V. Zenkina, A.B. McLean, B. Drevniok, Z. She, H.-B. Kraatz, N.J. Mosey, T. Seki, E.C. Keske, J.D. Leake, A. Rousina-Webb, G. Wu, Nat. Chem. 6 (2014) 409–414.
[34] J. Liu, P. Ruffieux, X. Feng, K. Mullen, R. Fasel, Chem. Commun. 50 (2014) 11200–11203.
[35] H. Zhou, J. Liu, S. Du, L. Zhang, G. Li, Y. Zhang, B.Z. Tang, H.-J. Gao, J. Am. Chem. Soc. 136 (2014) 5567–5570.
[36] Q. Sun, L. Cai, S. Wang, R. Widmer, H. Ju, J. Zhu, L. Li, Y. He, P. Ruffieux, R. Fasel, W. Xu, J. Am. Chem. Soc. 138 (2016) 1106–1109.
[37] F. Bebensee, C. Bombis, S.-R. Vadapoo, J.R. Cramer, F. Besenbacher, K.V. Gothelf, T.R. Linderoth, J. Am. Chem. Soc. 135 (2013) 2136–2139.
[38] O. Díaz Arado, H. Mönig, H. Wagner, J.-H. Franke, G. Langewisch, P.A. Held, A. Studer, H. Fuchs, ACS Nano 7 (2013) 8509–8515.
[39] V.K. Kanuru, G. Kyriakou, S.K. Beaumont, A.C. Papageorgiou, D.J. Watson, R.M. Lambert, J. Am. Chem. Soc. 132 (2010) 8081–8086.
[40] C. Sánchez-Sánchez, F. Yubero, A.R. González-Elipe, L. Feria, J.F. Sanz, R.M. Lambert, J. Phys. Chem. C 118 (2014) 11677–11684.
[41] Q. Sun, L. Cai, H. Ma, C. Yuan, W. Xu, ACS Nano 10 (2016) 7023–7030.
[42] J. Cai, P. Ruffieux, R. Jaafar, M. Bieri, T. Braun, S. Blankenburg, M. Muoth, A.P. Seitsonen, M. Saleh, X. Feng, K. Mullen, R. Fasel, Nature 466 (2010) 470–473.
[43] Q. Sun, C. Zhang, H. Kong, Q. Tan, W. Xu, Chem. Commun. 50 (2014) 11825–11828.
[44] Q. Sun, L. Cai, Y. Ding, L. Xie, C. Zhang, Q. Tan, W. Xu, Angew. Chem. Int. Ed. 54 (2015) 4549–4552.
[45] Q. Sun, L. Cai, H. Ma, C. Yuan, W. Xu, Chem. Commun. 52 (2016) 6009–6012.
[46] Q. Sun, L. Cai, Y. Ding, H. Ma, C. Yuan, W. Xu, Phys. Chem. Chem. Phys. 18 (2016) 2730–2735.
[47] D. Zhong, J.-H. Franke, S.K. Podiyanachari, T. Bloemker, H. Zhang, G. Kehr, G. Erker, H. Fuchs, L. Chi, Science 334 (2011) 213–216.
[48] H.-Y. Gao, P.A. Held, M. Knor, C. Mück-Lichtenfeld, J. Neugebauer, A. Studer, H. Fuchs, J. Am. Chem. Soc. 136 (2014) 9658–9663.
[49] P.A. Held, H.-Y. Gao, L. Liu, C. Mück-Lichtenfeld, A. Timmer, H. Mönig, D. Barton, J. Neugebauer, H. Fuchs, A. Studer, Angew. Chem. Int. Ed. 55 (2016) 9777–9782.
[50] B. Yang, J. Björk, H. Lin, X. Zhang, H. Zhang, Y. Li, J. Fan, Q. Li, L. Chi, J. Am. Chem. Soc. 137 (2015) 4904–4907.
[51] B. Yang, H. Lin, K. Miao, P. Zhu, L. Liang, K. Sun, H. Zhang, J. Fan, V. Meunier, Y. Li, Q. Li, L. Chi, Angew. Chem. 128 (2016) 10035–10039.
[52] J. Krüger, N. Pavliček, J.M. Alonso, D. Pérez, E. Guitián, T. Lehmann, G. Cuniberti, A. Gourdon, G. Meyer, L. Gross, F. Moresco, D. Peña, ACS Nano 10 (2016) 4538–4542.
[53] C.-Z. Guan, D. Wang, L.-J. Wan, Chem. Commun. 48 (2012) 2943–2945.
[54] L. Dong, Z.A. Gao, N. Lin, Progr. Surf. Sci. 91 (2016) 101–135.
[55] R. Gutzler, S. Stepanow, D. Grumelli, M. Lingenfelder, K. Kern, Acc. Chem. Res. 48 (2015) 2132–2139.
[56] X.-H. Liu, C.-Z. Guan, D. Wang, L.-J. Wan, Adv. Mater. 26 (2014) 6912–6920.
[57] J.C. Love, L.A. Estroff, J.K. Kriebel, R.G. Nuzzo, G.M. Whitesides, Chem. Rev. 105 (2005) 1103–1170.
[58] B.D. Gates, Q. Xu, M. Stewart, D. Ryan, C.G. Willson, G.M. Whitesides, Chem. Rev. 105 (2005) 1171–1196.
[59] H.-Y. Gao, J.-H. Franke, H. Wagner, D. Zhong, P.-A. Held, A. Studer, H. Fuchs, J. Phys. Chem. C 117 (2013) 18595–18602.
[60] J. Liu, Q. Chen, L. Xiao, J. Shang, X. Zhou, Y. Zhang, Y. Wang, X. Shao, J. Li, W. Chen, G.Q. Xu, H. Tang, D. Zhao, K. Wu, ACS Nano 9 (2015) 6305–6314.
[61] H.-Y. Gao, D. Zhong, H. Mönig, H. Wagner, P.-A. Held, A. Timmer, A. Studer, H. Fuchs, J. Phys. Chem. C 118 (2014) 6272–6277.
[62] S.-W. Hla, L. Bartels, G. Meyer, K.-H. Rieder, Phys. Rev. Lett. 85 (2000) 2777–2780.
[63] S.A. Krasnikov, C.M. Doyle, N.N. Sergeeva, A.B. Preobrajenski, N.A. Vinogradov, Y.N. Sergeeva, A.A. Zakharov, M.O. Senge, A.A. Cafolla, Nano Res. 4 (2011) 376–384.
[64] T. Lin, X.S. Shang, J. Adisoejoso, P.N. Liu, N. Lin, J. Am. Chem. Soc. 135 (2013) 3576–3582.
[65] A. Saywell, J. Schwarz, S. Hecht, L. Grill, Angew. Chem. Int. Ed. 51 (2012) 5096–5100.
[66] M. Koch, M. Gille, A. Viertel, S. Hecht, L. Grill, Surf. Sci. 627 (2014) 70–74.
[67] Q. Fan, C. Wang, Y. Han, J. Zhu, J. Kuttner, G. Hilt, J.M. Gottfried, ACS Nano 8 (2014) 709–718.
[68] Q. Fan, J. Dai, T. Wang, J. Kuttner, G. Hilt, J.M. Gottfried, J. Zhu, ACS Nano 10 (2016) 3747–3754.
[69] M. Chen, J. Shang, Y. Wang, K. Wu, J. Kuttner, G. Hilt, W. Hieringer, J.M. Gottfried, ACS Nano 11 (2017) 134–143.
[70] H. Zhang, Z. Gong, K. Sun, R. Duan, P. Ji, L. Li, C. Li, K. Müllen, L. Chi, J. Am. Chem. Soc. 138 (2016) 11743–11748.
[71] C. Bombis, F. Ample, L. Lafferentz, H. Yu, S. Hecht, C. Joachim, L. Grill, Angew. Chem. Int. Ed. 48 (2009) 9966–9970.
[72] M. Kolmer, A.A. Ahmad Zebari, J.S. Prauzner-Bechcicki, W. Piskorz, F. Zasada, S. Godlewski, B. Such, Z. Sojka, M. Szymonski, Angew. Chem. Int. Ed. 52 (2013) 10300–10303.
[73] Y. Bao, M. Yang, S.J.R. Tan, Y.P. Liu, H. Xu, W. Liu, C.T. Nai, Y.P. Feng, J. Lu, K.P. Loh, J. Am. Chem. Soc. 138 (2016) 14121–14128.
[74] S. Haq, F. Hanke, J. Sharp, M. Persson, D.B. Amabilino, R. Raval, ACS Nano 8 (2014) 8856–8870.
[75] J.V. Barth, Surf. Sci. 603 (2009) 1533–1541.
[76] G. Binnig, H. Rohrer, C. Gerber, E. Weibel, Phys. Rev. Lett. 49 (1982) 57–61.
[77] G. Binnig, C.F. Quate, C. Gerber, Phys. Rev. Lett. 56 (1986) 930–933.
[78] F.J. Giessibl, Rev. Mod. Phys. 75 (2003) 949–983.
[79] M. Ternes, C.P. Lutz, C.F. Hirjibehedin, F.J. Giessibl, A.J. Heinrich, Science 319 (2008) 1066–1069.
[80] N. Pavliček, B. Schuler, S. Collazos, N. Moll, D. Pérez, E. Guitián, G. Meyer, D. Peña, L. Gross, Nat. Chem. 7 (2015) 623–628.
[81] S. Kawai, V. Haapasilta, B.D. Lindner, K. Tahara, P. Spijker, J.A. Buitendijk, R. Pawlak, T. Meier, Y. Tobe, A.S. Foster, E. Meyer, Nat. Commun. 7 (2016) 12711.
[82] N. Kocić, X. Liu, S. Chen, S. Decurtins, O. Krejčí, P. Jelínek, J. Repp, S.-X. Liu, J. Am. Chem. Soc. 138 (2016) 5585–5593.
[83] J. Liu, T. Dienel, J. Liu, O. Groening, J. Cai, X. Feng, K. Müllen, P. Ruffieux, R. Fasel, J. Phys. Chem. C 120 (2016) 17588–17593.
[84] A. Riss, S. Wickenburg, P. Gorman, L.Z. Tan, H.-Z. Tsai, D.G. de Oteyza, Y.-C. Chen, A.J. Bradley, M.M. Ugeda, G. Etkin, S.G. Louie, F.R. Fischer, M.F. Crommie, Nano Lett. 14 (2014) 2251–2255.
[85] Z. Majzik, A.B. Cuenca, N. Pavliček, N. Miralles, G. Meyer, L. Gross, E. Fernández, ACS Nano 10 (2016) 5340–5345.
[86] L. Gross, F. Mohn, N. Moll, P. Liljeroth, G. Meyer, Science 325 (2009) 1110–1114.
[87] F. Albrecht, N. Pavliček, C. Herranz-Lancho, M. Ruben, J. Repp, J. Am. Chem. Soc. 137 (2015) 7424–7428.
[88] Z. Sun, M.P. Boneschanscher, I. Swart, D. Vanmaekelbergh, P. Liljeroth, Phys. Rev. Lett. 106 (2011) 046104.
[89] N. Moll, B. Schuler, S. Kawai, F. Xu, L. Peng, A. Orita, J. Otera, A. Curioni, M. Neu, J. Repp, G. Meyer, L. Gross, Nano Lett. 14 (2014) 6127–6131.
[90] S.K. Hämäläinen, N. van der Heijden, J. van der Lit, S. den Hartog, P. Liljeroth, I. Swart, Phys. Rev. Lett. 113 (2014) 186102.
[91] F. Mohn, B. Schuler, L. Gross, G. Meyer, Appl. Phys. Lett. 102 (2013) 073109.
[92] H. Mönig, D.R. Hermoso, O. Díaz Arado, M. Todorović, A. Timmer, S. Schüer, G. Langewisch, R. Pérez, H. Fuchs, ACS Nano 10 (2016) 1201–1209.
[93] M.A. Reed, Mater. Today 11 (2008) 46–50.
[94] T. Schmid, L. Opilik, C. Blum, R. Zenobi, Angew. Chem. Int. Ed. 52 (2013) 5940–5954.
[95] M.D. Sonntag, E.A. Pozzi, N. Jiang, M.C. Hersam, R.P. Van Duyne, J. Phys. Chem. Lett. 5 (2014) 3125–3130.
[96] Z. Zhang, S. Sheng, R. Wang, M. Sun, Anal. Chem. 88 (2016) 9328–9346.
[97] T.L. Cocker, D. Peller, P. Yu, J. Repp, R. Huber, Nature 539 (2016) 263–267.
[98] A. Basagni, F. Sedona, C.A. Pignedoli, M. Cattelan, L. Nicolas, M. Casarin, M. Sambi, J. Am. Chem. Soc. 137 (2015) 1802–1808.
[99] R.R. Cloke, T. Marangoni, G.D. Nguyen, T. Joshi, D.J. Rizzo, C. Bronner, T. Cao, S.G. Louie, M.F. Crommie, F.R. Fischer, J. Am. Chem. Soc. 137 (2015) 8872–8875.
[100] Y.-C. Chen, T. Cao, C. Chen, Z. Pedramrazi, D. Haberer, G. de OteyzaDimas, F.R. Fischer, S.G. Louie, M.F. Crommie, Nat. Nano 10 (2015) 156–160.
[101] M. Koch, F. Ample, C. Joachim, L. Grill, Nat. Nano 7 (2012) 713–717.
[102] S. Kawai, A. Benassi, E. Gnecco, H. Söde, R. Pawlak, X. Feng, K. Müllen, D. Passerone, C.A. Pignedoli, P. Ruffieux, R. Fasel, E. Meyer, Science 351 (2016) 957–961.

[103] J. Bjork, J. Phys.: Condens. Matter 28 (2016) 083002.
[104] S. Zhang, L. Nguyen, Y. Zhu, S. Zhan, C.-K. Tsung, F. Tao, Acc. Chem. Res. 46 (2013) 1731–1739.
[105] F. Tao, P.A. Crozier, Chem. Rev. 116 (2016) 3487–3539.
[106] J. Campos-Delgado, J.M. Romo-Herrera, X. Jia, D.A. Cullen, H. Muramatsu, Y.A. Kim, T. Hayashi, Z. Ren, D.J. Smith, Y. Okuno, T. Ohba, H. Kanoh, K. Kaneko, M. Endo, H. Terrones, M.S. Dresselhaus, M. Terrones, Nano Lett. 8 (2008) 2773–2778.
[107] S.S. Datta, D.R. Strachan, S.M. Khamis, A.T.C. Johnson, Nano Lett. 8 (2008) 1912–1915.
[108] X. Li, X. Wang, L. Zhang, S. Lee, H. Dai, Science 319 (2008) 1229–1232.
[109] M.Y. Han, B. Özyilmaz, Y. Zhang, P. Kim, Phys. Rev. Lett. 98 (2007) 206805.
[110] L. Tapaszto, G. Dobrik, P. Lambin, L.P. Biro, Nat. Nano 3 (2008) 397–401.
[111] L. Jiao, L. Zhang, X. Wang, G. Diankov, H. Dai, Nature 458 (2009) 877–880.
[112] L. Talirz, H. Söde, J. Cai, P. Ruffieux, S. Blankenburg, R. Jafaar, R. Berger, X. Feng, K. Müllen, D. Passerone, R. Fasel, C.A. Pignedoli, J. Am. Chem. Soc. 135 (2013) 2060–2063.
[113] S. Linden, D. Zhong, A. Timmer, N. Aghdassi, J.H. Franke, H. Zhang, X. Feng, K. Müllen, H. Fuchs, L. Chi, H. Zacharias, Phys. Rev. Lett. 108 (2012) 216801.
[114] A. Kimouche, M.M. Ervasti, R. Drost, S. Halonen, A. Harju, P.M. Joensuu, J. Sainio, P. Liljeroth, Nat. Commun. 6 (2015) 10177.
[115] H. Zhang, H. Lin, K. Sun, L. Chen, Y. Zagranyarski, N. Aghdassi, S. Duhm, Q. Li, D. Zhong, Y. Li, K. Müllen, H. Fuchs, L. Chi, J. Am. Chem. Soc. 137 (2015) 4022–4025.
[116] P. Ruffieux, S. Wang, B. Yang, C. Sánchez-Sánchez, J. Liu, T. Dienel, L. Talirz, P. Shinde, C.A. Pignedoli, D. Passerone, T. Dumslaff, X. Feng, K. Müllen, R. Fasel, Nature 531 (2016) 489–492.
[117] H. Sakaguchi, S. Song, T. Kojima, T. Nakae, Nat. Chem. 9 (2017) 57–63.
[118] Y.-C. Chen, D.G. de Oteyza, Z. Pedramrazi, C. Chen, F.R. Fischer, M.F. Crommie, ACS Nano 7 (2013) 6123–6128.
[119] J. Cai, C.A. Pignedoli, L. Talirz, P. Ruffieux, H. Söde, L. Liang, V. Meunier, R. Berger, R. Li, X. Feng, K. Müllen, R. Fasel, Nat. Nano 9 (2014) 896–900.
[120] Y. He, M. Garnica, F. Bischoff, J. Ducke, M.-L. Bocquet, M. Batzill, W. Auwärter, J.V. Barth, Nat. Chem. 9 (2017) 33–38.
[121] M. Feng, H. Sun, J. Zhao, H. Petek, ACS Nano 8 (2014) 8644–8652.
[122] M. Feng, H. Petek, Y. Shi, H. Sun, J. Zhao, F. Calaza, M. Sterrer, H.-J. Freund, ACS Nano 9 (2015) 12124–12136.
[123] J. Čechal, C.S. Kley, R. Pétuya, F. Schramm, M. Ruben, S. Stepanow, A. Arnau, K. Kern, J. Phys. Chem. C 120 (2016) 18622–18630.
[124] M. Pivetta, G.E. Pacchioni, U. Schlickum, J.V. Barth, H. Brune, Phys. Rev. Lett. 110 (2013) 086102.
[125] S. Nowakowska, A. Wäckerlin, S. Kawai, T. Ivas, J. Nowakowski, S. Fatayer, C. Wäckerlin, T. Nijs, E. Meyer, J. Björk, M. Stöhr, L.H. Gade, T.A. Jung, Nat. Commun. 6 (2015) 6071.
[126] S. Stepanow, M. Lingenfelder, A. Dmitriev, H. Spillmann, E. Delvigne, N. Lin, X. Deng, C. Cai, J.V. Barth, K. Kern, Nat. Mater. 3 (2004) 229–233.
[127] D. Kühne, F. Klappenberger, W. Krenner, S. Klyatskaya, M. Ruben, J.V. Barth, Proc. Natl. Acad. Sci. U. S. A. 107 (2010) 21332–21336.
[128] Q. Zhang, G. Kuang, R. Pang, X. Shi, N. Lin, ACS Nano 9 (2015) 12521–12528.
[129] N.J. Tao, Nat. Nano 1 (2006) 173–181.
[130] C. Nacci, F. Ample, D. Bleger, S. Hecht, C. Joachim, L. Grill, Nat. Commun. 6 (2015) 7397.
[131] G. Kuang, S.-Z. Chen, W. Wang, T. Lin, K. Chen, X. Shang, P.N. Liu, N. Lin, J. Am. Chem. Soc. 138 (2016) 11140–11143.
[132] G. Reecht, H. Bulou, F. Scheurer, V. Speisser, F. Mathevet, C. González, Y.J. Dappe, G. Schull, J. Phys. Chem. Lett. 6 (2015) 2987–2992.
[133] S. Kawai, M. Koch, E. Gnecco, A. Sadeghi, R. Pawlak, T. Glatzel, J. Schwarz, S. Goedecker, S. Hecht, A. Baratoff, L. Grill, E. Meyer, Proc. Natl. Acad. Sci. U. S. A. 111 (2014) 3968–3972.
[134] M.C. Chong, G. Reecht, H. Bulou, A. Boeglin, F. Scheurer, F. Mathevet, G. Schull, Phys. Rev. Lett. 116 (2016) 036802.
[135] A. DiLullo, S.-H. Chang, N. Baadji, K. Clark, J.-P. Klöckner, M.-H. Prosenc, S. Sanvito, R. Wiesendanger, G. Hoffmann, S.-W. Hla, Nano Lett. 12 (2012) 3174–3179.
[136] Z. Chen, W. Zhang, C.-A. Palma, A. Lodi Rizzini, B. Liu, A. Abbas, N. Richter, L. Martini, X.-Y. Wang, N. Cavani, H. Lu, N. Mishra, C. Coletti, R. Berger, F. Klappenberger, M. Kläui, A. Candini, M. Affronte, C. Zhou, V. De Renzi, U. del Pennino, J.V. Barth, H.J. Räder, A. Narita, X. Feng, K. Müllen, J. Am. Chem. Soc. 138 (2016) 15488–15496.
[137] S. Fabris, S. Stepanow, N. Lin, P. Gambardella, A. Dmitriev, J. Honolka, S. Baroni, K. Kern, Nano Lett. 11 (2011) 5414–5420.
[138] V. Navarro, M.A. van Spronsen, J.W.M. Frenken, Nat. Chem. 8 (2016) 929–934.

Qian Shen received her B.S. in chemistry from China Agriculture University in 2008 and her Ph.D. in physical chemistry from Peking University in 2013. She was a research fellow at National University of Singapore from 2013 to 2015. She is currently an associate professor at Institute of Advanced Materials (IAM), Nanjing Tech University, China. From 2016, she joined Prof. Dr. H. Fuchs group as a visiting scholar. Her current research interest is mainly about self-assembly and on-surface synthesis.

Hong-Ying Gao received his B. S. in physics and Ph.D. in chemistry from University of Science and Technology of China (USTC). Since 2011, he joined Prof. Harald Fuchs group as a postdoctoral fellow and received the Alexander Humboldt Fellowship (2012.6–2014.2). Now, he is a junior group leader and his current research interests focus on-surface synthesis, metal surface catalysis and STM induced luminescence.

Harald Fuchs is a Chair-Professor of Experimental Physics at the University of Münster, Germany. He spent from 1984 to 1985 a post-doctoral year with IBM Research Laboratory Zurich in the group of G. Binnig and H. Rohrer. From 1985 to 1993, he was heading the 'Ultrathin Organic Films' project with BASF AG, Germany, before he became in 1993 a Full Professor and Director of the Physical Institute of the University of Münster. He is the founder of the Center for nanotechnology (CeNTech) in Münster and its scientific director since 1993. His research focuses on nanoscale science and nanotechnology, ranging from scanning probe microscopy to self-organized nanostructure fabrication, on-surface chemical reactions, and nano-bio systems. He is an elected member of the German National Academy of Science 'Leopoldina', the German National Academy of Science and Engineering 'acatech', and the 'TWAS'.